Elastic behavior of disclination dipole near nanotube with surface/interface effect*

Zhao Ying-Xin(赵迎新)[a)†], Zeng Xin(曾 鑫)[a)], and Chen Chang-Ping(陈昌萍)[b)]

[a)] *State Key Laboratory of Advanced Design and Manufacturing for Vehicle Body, Hunan University, Changsha* 410082, *China*
[b)] *College of Civil Engineering and Architecture, Xiamen University of Technology, Xiamen* 361024, *China*

(Received 8 May 2013; revised manuscript received 18 July 2013; published online 24 January 2014)

In this paper, we present an analytical solution of the interaction of the nanotube (NT) with a wedge disclination dipole in nanotube-based composites. The corresponding boundary value problem is solved exactly by using complex potential functions. The explicit expression of the force exerted on disclination dipole is given by using the generalized Peach–Koehler formula. As a numerical illustration, both the equilibrium position and the stability of the disclination dipole are evaluated for different material combinations, relative thickness of an NT, surface/interface effects, and the features of the disclination dipole. The results show that as the thickness of the NT layer increases, the NT has a relatively major role in the force acting on the disclination dipole in the NT-based composite. The cooperative effect of surface/interface stresses and the NT becomes considerable as the increase of NT layer thickness. The equilibrium position may occur, even more than one, due to the influences of the surface/interface stress and the NT thickening. The influences of the surface/interface stresses and the thickness of the NT layer on the force are greatly dependent on the disclination angle.

Keywords: nanotube-based composites, disclination dipole, nanotube thickness, surface/interface effect

PACS: 02.30.Fn, 61.72.–y, 68.35.Gy, 61.46.Np **DOI:** 10.1088/1674-1056/23/3/030202

1. Introduction

In composite materials, where we combine distinct phases together for fillers, the opportunity exists to design materials for specific properties at various levels of scale.[1] Nanotubes (NTs), the synthesized atomic resolution characterizing nanoscale one-dimensional (1D) structures, are cylindrical hollow tubes, similar in diameter to biological ion channels (a few nanometers). Certainly, the exceptional effect of NTs as fillers should improve markedly as their fibers become smaller, because of the increased surface area (per volume of filler) available for the interaction with the matrix. For example, a NT of about 10 nm in diameter has an interfacial area with a matrix that is almost 1000 times greater than that of a 10-micrometre fiber of the same volume. This intimate contact can influence the properties of the matrix, and affect its chain entanglements, its morphology and even its crystallinity. In recent years there have been rapid advances in technology for synthesizing NTs made from various materials and modifying their surface chemical components, such as carbon and silicon carbide,[2–5] boron nitride (BN),[6–8] and titanium dioxide (TiO_2).[9,10] Therefore, NTs can be used as excellent nanofillers in diverse multifunctional composites to improve physical, mechanical, and electronic properties, and chemical capillarity, storage, and grafting properties of the composites unattainable from current materials.[11–16]

Disclinations were firstly defined by Volterra[17] and originally introduced in the mechanics of deformed solids. The disclinations, similar to dislocations, are defects with long-range distortion fields.[18] As is well known, a dislocation is determined by its Burgers vector $\boldsymbol{b}$. In the same manner, a disclination is related to an axial vector $\boldsymbol{\omega}$ (the Frank vector). For a single straight-linear disclination, the energies of self-screened disclination configurations (disclination dipoles, disclination loops, etc.) may be relatively small, and as proposed by Romanov,[19] the self-screened disclinations may exist more easily in bulk crystalline and/or amorphous solids. Self-screened disclination configurations can be directly observed in severely deformed solids.[20] They have been recognized as typical defects and the sources of characteristic singularities in the fields of displacement and rotation.[21–23] Disclinations are special physical objects that serve as carriers of violation of rotational symmetry.[24] They are found in nature and are used to describe such diverse phenomena as the arrangement of molecules in liquid crystals,[25] the deformation behaviors of metals,[26] the polarization effect and diffraction of electromagnetic waves,[27] the displacements of the Earth's crust,[28] galactic structures,[29] misorientation in heteroepitaxial diamond films,[30] etc. Moreover, comprehensive physical descriptions of plastic deformation of nanocrystalline material and its effect on mechanical properties of nanocrystalline material require the introduction of an adequate model given by the concept of disclinations to

*Project supported by the National Natural Science Foundation of China (Grant Nos. 11172094 and 11172095), the Program for New Century Excellent Talents in University of Ministry of Education of China (Grant No. NCET-11-0122), and the Hunan Provincial Natural Science Foundation for Creative Research Groups, China (Grant No. 12JJ7001).

†Corresponding author. E-mail: zhaoyx565@163.com

© 2014 Chinese Physical Society and IOP Publishing Ltd

explain the structural evolution and transitions among various substructures on various length scales.[31,32] In the early 1980s, the advent of the first nanocrystalline material[33,34] aroused a great interest in disclinations as a powerful mean to describe the structural and mechanical behaviors of nano-objects.[35] The geometric and elastic properties of wedge disclinations were used to model the pentagonal symmetry and strained state in nanoparticles,[36,37] to explain the abnormal Hall–Petch relation[38] and all kinds of grain boundary phenomena[39–43] in nanocrystalline materials, to study possible ways of misfit-strain accommodation in heterogeneous nano-layered structures,[44,45] etc. Accordingly, the disclination concept is recognized to be very helpful in various branches of physics and is significantly used to describe the structures and mechanical properties and to explain a variety of physical phenomena in solids.

As we have seen, the problems of edge and screw dislocations interacting with the NT accounting for the surface effects have been addressed by Shodja *et al.*[46] and Moeini–Ardakani *et al.*,[47] while the influence of NT on disclination defect behavior has not been quantitatively studied well. The focus of this research is to suggest a theoretical model to investigate the fundamental mechanism of the structure/size effect of NTs on wedge disclination dipoles in NT-based composites. Taking into account the nanoscale features of NTs, the Gurtin–Murdoch surface/interface elasticity model[48,49] is used to account for the surface/interface effect of the NTs. By utilizing this surface/interface elasticity model, great effort has been recently made to understand some unusual phenomena related to the surface/interface stresses in nanocomposites.[50–57]

The main work is to address the influences of different material combinations, relative thickness values of NTs and surface/interface effects as well as the features of the disclination dipole on the equilibrium position and the stability of the disclination dipole. Results from our micromechanical modeling show that the properties of NT-based composites are strongly influenced by the NT diameter. The importance of taking into account the surface/interface effects on disclination defect is highlighted in our characterization and modeling of model NT-based composites.

2. Problem solutions

In surface/interface elasticity theory, a surface or interface is regarded as a negligibly thin layer adhered to the underlying bulk material without slipping and having elastic constants different from those of its bulk counterpart. The surface stress tensor σ^{s} is related to the deformation dependent surface energy $\Pi\left(\varepsilon_{\alpha\beta}\right)$ by

$$\sigma^{\mathrm{s}}_{\alpha\beta} = \tau^{\mathrm{s}}\delta_{\alpha\beta} + \frac{\partial \Pi\left(\varepsilon_{\alpha\beta}\right)}{\partial \varepsilon_{\alpha\beta}}, \tag{1}$$

where $\varepsilon_{\alpha\beta}$ is the 2×2 strain tensor for surface/interface, $\delta_{\alpha\beta}$ represents the Kronecker delta for surface/interface and τ^{s} is the residual surface/interface tension.

The presence of surface/interface stress gives rise to a nonclassical boundary condition, which is in combination with the surface/interface stress–strain relations and the equations of classical elasticity forms a coupled system of field equations. From Gurtin and Murdoch[48] and Gurtin *et al.*,[49] on the assumption that the surface adheres to the bulk without slipping, and in the absence of body forces, the equilibrium and constitutive equations for the isotropic case can be summarized as follows. In the bulk

$$\begin{aligned} &\sigma^{\mathrm{b}}_{ij,j} = 0, \\ &\sigma^{\mathrm{b}}_{ij} = C_{ijkl}\varepsilon_{kl} = \left[\lambda\delta_{ij}\delta_{kl} + \mu\left(\delta_{ik}\delta_{jl} + \delta_{il}\delta_{jk}\right)\right]\varepsilon_{kl}, \end{aligned} \tag{2}$$

at the surface/interface

$$\left\langle \sigma^{\mathrm{b}}_{\beta\alpha} n_\alpha \right\rangle + \sigma^{\mathrm{s}}_{\beta\alpha,\beta} = 0, \quad \left\langle \sigma^{\mathrm{b}}_{ji} n_j n_i \right\rangle = \sigma^{\mathrm{s}}_{\alpha\beta}\kappa_{\alpha\beta}, \tag{3}$$

$$\sigma^{\mathrm{s}}_{\beta\alpha} = \tau^{\mathrm{s}}\delta_{\beta\alpha} + 2\left(\mu^{\mathrm{s}} - \tau^{\mathrm{s}}\right)\varepsilon_{\gamma\alpha}\delta_{\beta\gamma} + \left(\lambda^{\mathrm{s}} + \tau^{\mathrm{s}}\right)\varepsilon_{\gamma\gamma}\delta_{\beta\alpha}, \tag{4}$$

where λ and μ are the Lamé constants for the isotropic bulk material. Isotropic interfaces or surfaces can be characterized by surface/interface Lamé constants μ^{s} and λ^{s} (which render the surface/interface energy deformation dependent) and residual surface/interface tension τ^{s} (under unstrained conditions). The superscripts b and s denote the bulk and the surface/interface, respectively. Here $\kappa_{\alpha\beta}$ represents the curvature tensor of the surface or interface, n_α is the normal vector at the interface or surface and finally ε_{ij} is the infinitesimal strain tensor and σ_{ij} is the corresponding stress tensor. In addition, $\langle W\rangle = W_2 - W_1$ denotes the jump across the surface/interface from matrix to the NT.

It is noted that only certain strain components appear within the constitutive law for surface/interface due to the 2×2 nature of the surface/interface stress tensor (i.e., strains normal to the surface/interface are excluded). Thus, the Greek indices take on values 1 and 2 while Latin subscripts adopt values 1 through 3. Conventional summation rules are used unless otherwise noted.

Figure 1 shows the plane physical problem to be treated in this paper. An NT with inner radius R_1 and outer radius R_2 is filled into the infinite elastic matrix. The NT is straight and infinitely extended in a direction perpendicular to xOy plane. The circles Γ_1 and Γ_2 are used to denote the NT's inner surface and the outer NT-matrix interface, respectively. Perfect bonding conditions are assumed at the surface/interface Γ_1 and Γ_2. The NT and matrix are both assumed to be isotropically elastic with elastic properties μ_1, υ_1 and μ_2, υ_2. The origin of the rectangular coordinate is selected to be at the center of the circular NT. The wedge disclination dipole consists of a positive disclination with strength ω at $z_1(= x_1 + \mathrm{i}y_1 = z_0 - p\mathrm{e}^{\mathrm{i}\phi})$ and a negative disclination with

the same strength at z_2 $(= x_2 + \mathrm{i}y_2 = z_0 + p\mathrm{e}^{\mathrm{i}\varphi})$ in an infinite matrix, so that the dipole arm has the length $2p$ and $z_0 = \rho\,\mathrm{e}^{\mathrm{i}\theta}$. Both disclination lines are perpendicular to the xOy plane.

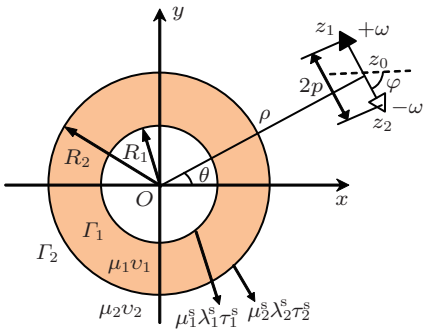


Fig. 1. (color online) A wedge disclination dipole in an NT-based composite.

For the present problem, based on Eqs. (3) and (4), the boundary conditions at the surface/interface Γ_1 and Γ_2 can be expressed as follows:

$$[\sigma_{rr1}(t) + \mathrm{i}\sigma_{r\theta 1}(t)]^- = \frac{1}{R_1}\left[\sigma^{\mathrm{s}}_{\theta\theta 1}(t) - \mathrm{i}\frac{\partial \sigma^{\mathrm{s}}_{\theta\theta 1}(t)}{\partial\theta}\right], \quad (5)$$

$$[u_{r1}(\zeta) + \mathrm{i}u_{\theta 1}(\zeta)]^+ = [u_{r2}(\zeta) + \mathrm{i}u_{\theta 2}(\zeta)]^-, \quad (6)$$

$$[\sigma_{rr2}(\zeta) + \mathrm{i}\sigma_{r\theta 2}(\zeta)]^- - [\sigma_{rr1}(\zeta) + \mathrm{i}\sigma_{r\theta 1}(\zeta)]^+ = \frac{1}{R_2}\left[\sigma^{\mathrm{s}}_{\theta\theta 1}(\zeta) - \mathrm{i}\frac{\partial \sigma^{\mathrm{s}}_{\theta\theta 1}(\zeta)}{\partial\theta}\right], \quad (7)$$

where $(\sigma_{rr},\ \sigma_{r\theta})$ and $(u_r,\ u_\theta)$ are the stress and displacement components, respectively, in the polar coordinates (r, θ) with the origin at the center of the circular NT, the superscripts "+" and "−" denote the boundary values of a physical quantity as z approaches the surface/interface from the interior and exterior of a circle, respectively. In addition, $|t| = R_1$ and $|\zeta| = R_2$.

In light of Muskhelishvili,[58] the bulk stress and displacement components can be expressed in terms of two complex potentials $u_5 = 0.01$ and $\Psi(z)$ of the complex variable z as follows:

$$\sigma_{yy} + \sigma_{xx} = 2\left[\Phi(z) + \overline{\Phi(z)}\right], \quad (8)$$

$$\sigma_{yy} - \sigma_{xx} + 2\mathrm{i}\sigma_{xy} = 2\left[\overline{z}\Phi'(z) - \Psi(z)\right], \quad (9)$$

$$2\mu\left(u'_x + u'_y\right) = \mathrm{i}z\left[\kappa\Phi(z) - \overline{\Phi(z)} + \overline{z}\overline{\Phi'(z)} + \frac{\overline{z}}{z}\overline{\Psi(z)}\right], \quad (10)$$

where σ_{xx}, σ_{yy}, and σ_{xy} are the stress components in Cartesian coordinates, $u'_x = \partial u_x/\partial\theta$, $u'_y = \partial u_y/\partial\theta$, u_x, and u_y are the displacement components, $\Phi'(z) = \mathrm{d}[\Phi(z)]/\mathrm{d}z$, $z = \rho\,\mathrm{e}^{\mathrm{i}\theta}$, the overbar represents the complex conjugate, and $\kappa = 3 - 4\upsilon$ for the plane strain state.

For a wedge disclination dipole placed inside the matrix, two complex potentials $\Phi_1(z)$ and $\Psi_1(z)$ which are holomorphic in the NT can be taken in the following forms:

$$\Phi_1(z) = \sum_{k=0}^{\infty} a_k z^k + \sum_{k=1}^{\infty} b_k z^{-k}, \quad (11)$$

$$\Psi_1(z) = \sum_{k=0}^{\infty} c_k z^{k-2} + \sum_{k=1}^{\infty} d_k z^{-k-2}, \quad (12)$$

where the unknown coefficients a_k, b_k, c_k, and d_k could be determined from the boundary conditions (5)–(7). For simplicity in the calculations, we assume that $T_P(z) = \sum_{k=0}^{\infty} a_k z^k$ and $T_N(z) = \sum_{k=1}^{\infty} b_k z^{-k}$.

According to Romanov and Vladimirov,[18] Liu *et al.*,[59] and Fang *et al.*,[60] two complex potentials $\Phi_2(z)$ and $\Psi_2(z)$ in the matrix can be represented as follows:

$$\Phi_2(z) = \frac{D_2\omega}{2}\left[\ln(z - z_1) - \ln(z - z_2)\right] + \Phi_{20}(z), \quad (13)$$

$$\Psi_2(z) = \frac{D_2\omega}{2}\left(\frac{\overline{z_2}}{z - z_2} - \frac{\overline{z_1}}{z - z_1}\right) + \Psi_{20}(z), \quad (14)$$

where $D_2 = \mu_2/[2\pi(1 - \upsilon_2)]$, $\Phi_{20}(z)$ and $\Psi_{20}(z)$ are holomorphic in the matrix.

To treat the boundary conditions at the surface/interface, it is convenient to introduce the following new analytical functions in the corresponding regions according to the Schwarz symmetry principle

$$\Phi_1^*(z) = -\overline{\Phi_1}\left(\frac{R_1^2}{z}\right) + \frac{R_1^2}{z}\overline{\Phi_1'}\left(\frac{R_1^2}{z}\right) + \frac{R_1^2}{z^2}\overline{\Psi_1}\left(\frac{R_1^2}{z}\right), \quad |z| < R_1, \quad (15)$$

$$\Phi_1^{**}(z) = -\overline{\Phi_1}\left(\frac{R_2^2}{z}\right) + \frac{R_2^2}{z}\overline{\Phi_1'}\left(\frac{R_2^2}{z}\right) + \frac{R_2^2}{z^2}\overline{\Psi_1}\left(\frac{R_2^2}{z}\right), \quad |z| > R_2, \quad (16)$$

$$\Phi_2^*(z) = -\overline{\Phi_2}\left(\frac{R_2^2}{z}\right) + \frac{R_2^2}{z}\overline{\Phi_2'}\left(\frac{R_2^2}{z}\right) + \frac{R_2^2}{z^2}\overline{\Psi_2}\left(\frac{R_2^2}{z}\right), \quad |z| < R_2. \quad (17)$$

Substituting Eqs. (11)–(14) into Eqs. (15)–(17), we have

$$\Phi_1^*(z) = F_N(z) + F_P(z), \quad (18)$$

$$\Phi_1^{**}(z) = H_N(z) + H_P(z), \quad (19)$$

$$\Phi_2^*(z) = \frac{D_2\omega}{2}\left(\ln\frac{z - z_2^*}{z - z_1^*} + \frac{z_1 - z_1^*}{z - z_1^*} - \frac{z_2 - z_2^*}{z - z_2^*} + \frac{z_2 - z_1}{z}\right) + \Phi_{20}^*(z), \quad (20)$$

where $z_1^* = R_2^2/\overline{z_1}$, $z_2^* = R_2^2/\overline{z_2}$,

$$F_N(z) = \sum_{k=1}^{\infty}\left[(k-1)\overline{a_k}R_1^{2k} + \overline{c_k}R_1^{2(k-1)}\right]z^{-k},$$

$$F_P(z) = -\overline{a_0} + \overline{c_0}R_1^{-2} + \sum_{k=1}^{\infty}\left[-(k+1)\overline{b_k}R_1^{-2k} + \overline{d_k}R_1^{-2(k+1)}\right]z^k,$$

$$H_N(z) = \sum_{k=1}^{\infty}\left[(k-1)\overline{a_k}R_2^{2k} + \overline{c_k}R_2^{2(k-1)}\right]z^{-k},$$

$$H_P(z) = -\overline{a_0} + \overline{c_0}R_2^{-2} + \sum_{k=1}^{\infty}\left[-(k+1)\overline{b_k}R_2^{-2k} + \overline{d_k}R_2^{-2(k+1)}\right]z^k,$$

and $\Phi_{20}^{*}(z)$ is holomorphic in the region $|z|<R_2$.

The surface/interfacial stress–strain relationship is given by Sharma[61] as

$$\sigma_{\theta\theta}^{\mathrm{s}}=\tau^{\mathrm{s}}+\left(2\mu^{\mathrm{s}}+\lambda^{\mathrm{s}}-\tau^{\mathrm{s}}\right)\varepsilon_{\theta\theta}^{\mathrm{s}}, \tag{21}$$

where $\sigma_{\theta\theta}^{\mathrm{s}}$ and $\varepsilon_{\theta\theta}^{\mathrm{s}}$ denote surface/interfacial stress and strain in the polar coordinates. Here, we consider a coherent interface. Thus surface/interface strain is equal to the associated tangential strain in the abutting bulk material.

In view of the above additional constitutive equation for the surface/interface region and the constitutive equation for the bulk solid and according to Fang *et al.*,[62] the stress discontinuity condition in Eq. (5) at the surface Γ_1 can be rewritten as

$$\begin{aligned}&\left[\sigma_{rr1}+\mathrm{i}\sigma_{r\theta1}\right]^{-}\\ =&\ \frac{\tau_1^{\mathrm{s}}}{R_1}+\frac{2\mu_1^{\mathrm{s}}+\lambda_1^{\mathrm{s}}-\tau_1^{\mathrm{s}}}{4R_1\mu_1}\\ &\times\left[\left(\sigma_{\theta\theta1}-\sigma_{rr1}\right)+\frac{\mu_1}{\lambda_1+\mu_1}\left(\sigma_{\theta\theta1}+\sigma_{rr1}\right)\right.\\ &\left.-\mathrm{i}\frac{\partial\left(\sigma_{\theta\theta1}-\sigma_{rr1}\right)}{\partial\theta}-\mathrm{i}\frac{\mu_1}{\lambda_1+\mu_1}\frac{\partial\left(\sigma_{\theta\theta1}+\sigma_{rr1}\right)}{\partial\theta}\right],\end{aligned} \tag{22}$$

where μ_1^{s} and λ_1^{s} are the surface constants, τ_1^{s} is the residual surface tension at the surface Γ_1.

With the help of Eqs. (8), (9), (11), and (18), equation (22) can be rewritten as

$$\begin{aligned}&\left[\left(1+\alpha_1\right)\Phi_1^{*}(t)+\alpha_1 t\Phi_1^{*'}(t)+\left(\alpha_1+\beta_1\right)\overline{\Phi_1}\left(\frac{R_1^2}{t}\right)\right.\\ &\left.-\left(\alpha_1+\beta_1\right)\frac{R_1^2}{t}\overline{\Phi_1'}\left(\frac{R_1^2}{t}\right)\right]^{+}\\ =&\left[\left(1-\alpha_1-\beta_1\right)\Phi_1(t)-\left(\alpha_1+\beta_1\right)t\Phi_1'(t)\right.\\ &\left.-\alpha_1\overline{\Phi_1^{*}}\left(\frac{R_1^2}{t}\right)+\alpha_1\frac{R_1^2}{t}\overline{\Phi_1^{*'}}\left(\frac{R_1^2}{t}\right)-\frac{\tau_1^{\mathrm{s}}}{R_1}\right]^{-},\end{aligned} \tag{23}$$

where $\alpha_1=(2\mu_1^{\mathrm{s}}+\lambda_1^{\mathrm{s}}-\tau_1^{\mathrm{s}})/(4R_1\mu_1)$

$$\beta_1=(2\mu_1^{\mathrm{s}}+\lambda_1^{\mathrm{s}}-\tau_1^{\mathrm{s}})/[2R_1(\lambda_1+\mu_1)].$$

Let

$$\begin{aligned}f_1(z)=&\left(1+\alpha_1\right)\Phi_1^{*}(z)+\alpha_1 z\Phi_1^{*'}(z)+\left(\alpha_1+\beta_1\right)\overline{\Phi_1}\left(\frac{R_1^2}{z}\right)\\ &-\left(\alpha_1+\beta_1\right)\frac{R_1^2}{z}\overline{\Phi_1'}\left(\frac{R_1^2}{z}\right),\quad |z|<R_1,\end{aligned} \tag{24}$$

$$\begin{aligned}f_1(z)=&\left(1-\alpha_1-\beta_1\right)\Phi_1(z)-\left(\alpha_1+\beta_1\right)z\Phi_1'(z)\\ &-\alpha_1\overline{\Phi_1^{*}}\left(\frac{R_1^2}{z}\right)+\alpha_1\frac{R_1^2}{z}\overline{\Phi_1^{*'}}\left(\frac{R_1^2}{z}\right)-\frac{\tau_1^{\mathrm{s}}}{R_1},\\ &R_1<|z|<R_2,\end{aligned} \tag{25}$$

by the use of the generalized Liouville theorem, then we have

$$\begin{aligned}f_1(z)=&\left(1+\alpha_1\right)F_N(z)+\alpha_1 zF_N'(z)+\left(\alpha_1+\beta_1\right)\overline{T_P}\left(\frac{R_1^2}{z}\right)\\ &-\left(\alpha_1+\beta_1\right)\frac{R_1^2}{z}\overline{T_P'}\left(\frac{R_1^2}{z}\right)\\ &+\left(1-\alpha_1-\beta_1\right)T_P(z)-\left(\alpha_1+\beta_1\right)zT_P'(z)\\ &-\alpha_1\overline{F_N}\left(\frac{R_1^2}{z}\right)+\alpha_1\frac{R_1^2}{z}\overline{F_N'}\left(\frac{R_1^2}{z}\right)-\frac{\tau_1^{\mathrm{s}}}{R_1}.\end{aligned} \tag{26}$$

Referring to Eq. (24), the following complex expression can be yielded as

$$\begin{aligned}\Phi_1^{*}(z)=&\frac{1}{1+\alpha_1}\left[f_1(z)-\alpha_1 z\Phi_1^{*'}(z)-\left(\alpha_1+\beta_1\right)\overline{\Phi_1}\left(\frac{R_1^2}{z}\right)\right.\\ &\left.+\left(\alpha_1+\beta_1\right)\frac{R_1^2}{z}\overline{\Phi_1'}\left(\frac{R_1^2}{z}\right)\right].\end{aligned} \tag{27}$$

Considering Eq. (25), the following complex expression can be obtained

$$\begin{aligned}\Phi_1(z)=&\frac{1}{1-\alpha_1-\beta_1}\left[f_1(z)+\left(\alpha_1+\beta_1\right)z\Phi_1'(z)\right.\\ &\left.+\alpha_1\overline{\Phi_1^{*}}\left(\frac{R_1^2}{z}\right)-\alpha_1\frac{R_1^2}{z}\overline{\Phi_1^{*'}}\left(\frac{R_1^2}{z}\right)+\frac{\tau_1^{\mathrm{s}}}{R_1}\right].\end{aligned} \tag{28}$$

The substitution of Eqs. (11), (18), and (26) into Eq. (28) yields

$$\begin{aligned}\Phi_1(z)=&w_1\left[e_1F_N(z)+e_2zF_N'(z)+e_3\overline{T_P}\left(\frac{R_1^2}{z}\right)\right.\\ &-e_3\frac{R_1^2}{z}\overline{T_P'}\left(\frac{R_1^2}{z}\right)+e_4T_P(z)+e_3zT_N'(z)\\ &\left.+e_2\overline{F_P}\left(\frac{R_1^2}{z}\right)-e_2\frac{R_1^2}{z}\overline{F_P'}\left(\frac{R_1^2}{z}\right)\right],\end{aligned} \tag{29}$$

where $w_1=1/(1-\alpha_1-\beta_1)$, $e_1=1+\alpha_1$, $e_2=\alpha_1$, $e_3=\alpha_1+\beta_1$, and $e_4=1-\alpha_1-\beta_1$.

Taking the complex conjugate of Eq. (15) and according to Eqs. (27)–(29), it is found that

$$\begin{aligned}\Psi_1(z)=&\frac{R_1^2}{z^2}\left\{s_1F_N(z)+s_2zF_N'(z)+s_3\overline{T_P}\left(\frac{R_1^2}{z}\right)\right.\\ &+s_4\frac{R_1^2}{z}\overline{T_P'}\left(\frac{R_1^2}{z}\right)+s_5T_P(z)+s_6zT_N'(z)\\ &+s_7\overline{F_P}\left(\frac{R_1^2}{z}\right)+s_8\frac{R_1^2}{z}\overline{F_P'}\left(\frac{R_1^2}{z}\right)\\ &-s_9z^{-2}+s_{10}\overline{F_N}\left(\frac{R_1^2}{z}\right)-s_6T_N(z)-s_{11}\\ &-s_7z^2F_N''(z)-s_{12}z\left[\overline{T_P}\left(\frac{R_1^2}{z}\right)\right]'\\ &+s_{12}R_1^2\left[\overline{T_P'}\left(\frac{R_1^2}{z}\right)\right]'-s_5zT_P'(z)-s_{12}z^2T_N''(z)\\ &\left.-s_7z\left[\overline{F_P}\left(\frac{R_1^2}{z}\right)\right]'+s_7R_1^2\left[\overline{F_P'}\left(\frac{R_1^2}{z}\right)\right]'\right\},\end{aligned} \tag{30}$$

where $s_1=w_1e_1-w_2e_2$, $s_2=w_1e_2+w_2e_2-w_1e_8$, $s_3=w_1e_3+w_2e_7$, $s_4=-2w_1e_3-w_2e_3$, $s_5=w_1e_4$, $s_6=w_2e_3$, $s_7=w_1e_2$, $s_8=-2w_1e_2-w_2e_2$, $s_9=w_2e_6$, $s_{10}=w_2\tau_1^{\mathrm{s}}/R_1$,

$s_{11}=w_1e_3$, $w_2=1/(1+\alpha_1)$, $e_5=1+\alpha_1$, $e_6=1-\alpha_1-\beta_1$, and $e_7=1+2\alpha_1$. Considering Eq. (10) and the displacement continuity condition on the entire circular interface Γ_2, equation (6) can be rewritten as

$$\left[\frac{\kappa_1}{\mu_1}\Phi_1(\zeta)-\frac{1}{\mu_2}\Phi_2^*(\zeta)\right]^+ = \left[\frac{\kappa_2}{\mu_2}\Phi_2(\zeta)-\frac{1}{\mu_1}\Phi_1^{**}(\zeta)\right]^-, \quad |\zeta|=R_2. \tag{31}$$

Let

$$F_2(z)=\frac{\kappa_1}{\mu_1}\Phi_1(z)-\frac{1}{\mu_2}\Phi_2^*(z), \quad R_1<|z|<R_2, \tag{32}$$

$$F_2(z)=\frac{\kappa_2}{\mu_2}\Phi_2(z)-\frac{1}{\mu_1}\Phi_1^{**}(z), \quad |z|>R_2, \tag{33}$$

using the generalized Liouville theorem, the following equation can be obtained:

$$\begin{aligned}F_2(z) = {} & \frac{\kappa_2}{\mu_2}\frac{D_2\omega}{2}\ln\frac{z-z_1}{z-z_2} \\ & -\frac{1}{\mu_2}\frac{D_2\omega}{2}\left(\ln\frac{z-z_2^*}{z-z_1^*}+\frac{z_1-z_1^*}{z-z_1^*}-\frac{z_2-z_2^*}{z-z_2^*}+\frac{z_2-z_1}{z}\right) \\ & +\frac{\kappa_1}{\mu_1}T_N(z)-\frac{1}{\mu_1}H_P(z).\end{aligned} \tag{34}$$

Utilizing a similar way to consider the stress discontinuity condition at the interface Γ_2, equation (7) can be rewritten as

$$\begin{aligned}&\left[\Phi_2(\zeta)+(1-\alpha_2)\Phi_1^{**}(\zeta)-\alpha_2\zeta\Phi_1^{**'}(\zeta)\right. \\ &\left.-(\alpha_2+\beta_2)\overline{\Phi_1}\left(\frac{R_2^2}{\zeta}\right)+(\alpha_2+\beta_2)\frac{R_2^2}{\zeta}\overline{\Phi_1'}\left(\frac{R_2^2}{\zeta}\right)-\frac{\tau_2^s}{R_2}\right]^- \\ = {} & \left[(1+\alpha_2+\beta_2)\Phi_1(\zeta)+\Phi_2^*(\zeta)+(\alpha_2+\beta_2)\zeta\Phi_1'(\zeta)\right. \\ &\left.+\alpha_2\overline{\Phi_1^{**}}\left(\frac{R_2^2}{\zeta}\right)-\alpha_2\frac{R_2^2}{\zeta}\overline{\Phi_1^{**'}}\left(\frac{R_2^2}{\zeta}\right)\right]^+, \quad |\zeta|=R_2,\end{aligned} \tag{35}$$

where

$$\alpha_2=(2\mu_2^s+\lambda_2^s-\tau_2^s)/(4R_2\mu_1),$$
$$\beta_2=(2\mu_2^s+\lambda_2^s-\tau_2^s)/[2R_2(\lambda_1+\mu_1)],$$

μ_2^s and λ_2^s are interface constants, τ_2^s is the residual interface tension at the interface Γ_2. Let

$$\begin{aligned}F_3(z) = {} & (1+\alpha_2+\beta_2)\Phi_1(z)+\Phi_2^*(z)+(\alpha_2+\beta_2)z\Phi_1'(z) \\ & +\alpha_2\overline{\Phi_1^{**}}\left(\frac{R_2^2}{z}\right)-\alpha_2\frac{R_2^2}{z}\overline{\Phi_1^{**'}}\left(\frac{R_2^2}{z}\right), \\ & R_1<|z|<R_2,\end{aligned} \tag{36}$$

$$\begin{aligned}F_3(z) = {} & \Phi_2(z)+(1-\alpha_2)\Phi_1^{**}(z)-\alpha_2z\Phi_1^{**'}(z) \\ & -(\alpha_2+\beta_2)\overline{\Phi_1}\left(\frac{R_2^2}{z}\right) \\ & +(\alpha_2+\beta_2)\frac{R_2^2}{z}\overline{\Phi_1'}\left(\frac{R_2^2}{z}\right)-\frac{\tau_2^s}{R_2}, \quad |z|>R_2,\end{aligned} \tag{37}$$

using the generalized Liouville theorem, then we have

$$\begin{aligned}F_3(z) = {} & \frac{D_2\omega}{2}\left(\ln\frac{z-z_2^*}{z-z_1^*}+\frac{z_1-z_1^*}{z-z_1^*}-\frac{z_2-z_2^*}{z-z_2^*}+\frac{z_2-z_1}{z}\right) \\ & +\frac{D_2\omega}{2}\ln\frac{z-z_1}{z-z_2}-\frac{\tau_2^s}{R_2} \\ & +(1+\alpha_2+\beta_2)T_N(z)+(\alpha_2+\beta_2)zT_N'(z) \\ & +\alpha_2\overline{H_P}\left(\frac{R_2^2}{z}\right)-\alpha_2\frac{R_2^2}{z}\overline{H_p'}\left(\frac{R_2^2}{z}\right) \\ & +(1-\alpha_2)H_P(z)-\alpha_2zH_p'(z)-(\alpha_2+\beta_2)\overline{T_N}\left(\frac{R_2^2}{z}\right) \\ & +(\alpha_2+\beta_2)\frac{R_2^2}{z}\overline{T_N'}\left(\frac{R_2^2}{z}\right).\end{aligned} \tag{38}$$

Combining Eqs. (32) and (36), we have

$$\begin{aligned}\Phi_1(z) = {} & \frac{1}{\mu_2\kappa_1/\mu_1+1+\alpha_2+\beta_2} \\ & \times\left[\mu_2F_2(z)+F_3(z)-(\alpha_2+\beta_2)z\Phi_1'(z)\right. \\ & \left.-\alpha_2\overline{\Phi_1^{**}}\left(\frac{R_2^2}{z}\right)+\alpha_2\frac{R_2^2}{z}\overline{\Phi_1^{**'}}\left(\frac{R_2^2}{z}\right)\right].\end{aligned} \tag{39}$$

Referring to Eqs. (33) and (37), we have

$$\begin{aligned}\Phi_1^{**}(z) = {} & \frac{1}{1-\alpha_2+\mu_2/\kappa_2\mu_1}\left[F_3(z)-\frac{\mu_2}{\kappa_2}F_2(z)+\alpha_2z\Phi_1^{**'}(z)\right. \\ & +(\alpha_2+\beta_2)\overline{\Phi_1}\left(\frac{R_2^2}{z}\right) \\ & \left.-(\alpha_2+\beta_2)\frac{R_2^2}{z}\overline{\Phi_1'}\left(\frac{R_2^2}{z}\right)+\frac{\tau_2^s}{R_2}\right].\end{aligned} \tag{40}$$

Substitution of Eqs. (11), (16), (34), and (38) into Eq. (39) yields

$$\begin{aligned}\Phi_1(z) = {} & w_3\left[f_1\ln\frac{z-z_1}{z-z_2}+f_2T_N(z)+f_3H_P(z)\right. \\ & -f_4zH_P'(z)-f_5\overline{T_N}\left(\frac{R_2^2}{z}\right) \\ & +f_5\frac{R_2^2}{z}\overline{T_N'}\left(\frac{R_2^2}{z}\right)-f_5zT_P'(z)-f_4\overline{H_N}\left(\frac{R_2^2}{z}\right) \\ & \left.+f_4\frac{R_2^2}{z}\overline{H_N'}\left(\frac{R_2^2}{z}\right)-\frac{\tau_2^s}{R_2}\right],\end{aligned} \tag{41}$$

where $w_3=1/(\mu_2\kappa_1/\mu_1+1+\alpha_2+\beta_2)$, $f_1=(\kappa_2+1)M$, $M=D_2\omega/2$, $f_2=\mu_2\kappa_1/\mu_1+1+\alpha_2+\beta_2$, $f_3=1-\alpha_2-\mu_2/\mu_1$, $f_4=\alpha_2$, and $f_5=\alpha_2+\beta_2$.

Taking the complex conjugate of Eq. (16) and according to Eqs. (11), (40), and (41), we can obtain that

$$\begin{aligned}\Psi_1(z) = {} & \frac{R_2^2}{z^2}\left\{t_1\ln\frac{z-z_1}{z-z_2}-t_2\frac{z}{z-z_1}+t_3\frac{z}{z-z_2}+t_4T_N(z)\right. \\ & +t_5H_P(z)+t_6zH_P'(z)+t_7\overline{T_N}\left(\frac{R_2^2}{z}\right) \\ & \left.+t_8\frac{R_2^2}{z}\overline{T_N'}\left(\frac{R_2^2}{z}\right)-t_9zT_P'(z)-t_{10}\overline{H_N}\left(\frac{R_2^2}{z}\right)\right.\end{aligned}$$

$$+t_{11}\frac{R_2^2}{z}\overline{H_N'}\left(\frac{R_2^2}{z}\right)-t_{12}+t_{13}z+t_{14}\overline{H_P}\left(\frac{R_2^2}{z}\right)$$
$$+t_9T_P(z)-t_4zT_N'(z)+t_{10}z^2H_P''(z)+t_{15}z\left[\overline{T_N}\left(\frac{R_2^2}{z}\right)\right]'$$
$$-t_{15}R_2^2\left[\overline{T_N'}\left(\frac{R_2^2}{z}\right)\right]'+t_{15}z^2T_P''(z)$$
$$+t_{10}z\left[\overline{H_N}\left(\frac{R_2^2}{z}\right)\right]'-t_{10}R_2^2\left[\overline{H_N'}\left(\frac{R_2^2}{z}\right)\right]'\Bigg\}, \quad (42)$$

where $t_1=w_3f_1-w_4f_6$, $t_2=w_4f_7+w_3f_1$, $t_3=w_4f_8+w_3f_1$, $t_4=w_3f_2$, $t_5=w_3f_3+w_4f_4$, $t_6=-w_4f_4-w_3f_3$, $t_7=-w_3f_5+w_4f_{10}$, $t_8=2w_3f_5+w_4f_5$, $t_9=w_4f_5$, $t_{10}=w_3f_4$, $t_{11}=2w_3f_4+w_4f_4$, $t_{12}=w_3\tau_2^0/R_2-w_4f_6\ln(z_1/z_2)$, $t_{13}=w_4f_9$, $t_{14}=w_4f_{11}$, $t_{15}=w_3f_5$, $w_4=\mu_2/(\kappa_2\mu_1)+1-\alpha_2$, $f_6=(1/\kappa_2+1)M$, $f_7=(1/\kappa_2+1)M(\overline{z_1}-\overline{z_1^*})/\overline{z_1^*}$, $f_8=(1/\kappa_2+1)M(\overline{z_2}-\overline{z_2^*})/\overline{z_2^*}$, $f_9=(1/\kappa_2+1)M(\overline{z_2}-\overline{z_1})/R_2^2$, $f_{10}=1+\alpha_2+\beta_2-\mu_2\kappa_1/\mu_1\kappa_2$, and $f_{11}=1-\alpha_2+\mu_2/\mu_1\kappa_2$.

In order to simultaneously satisfy all of the boundary conditions at the surface/interface Γ_1 and Γ_2, the two expressions of $\Phi_{10}(z)$ and $\Psi_{10}(z)$ obtained in the above part must be compatible with each other.[63–66] Physically, the compatibility conditions for $\Phi_{10}(z)$ and $\Psi_{10}(z)$ imply that the stress field and displacement field in the NT are unique.

Referring to Eqs. (29), (30), (41), and (42), we have

$$w_1\Bigg[e_1F_N(z)+e_2zF_N'(z)+e_3\overline{T_P}\left(\frac{R_1^2}{z}\right)-e_3\frac{R_1^2}{z}\overline{T_P'}\left(\frac{R_1^2}{z}\right)$$
$$+e_4T_P(z)+e_3zT_N'(z)+e_2\overline{F_P}\left(\frac{R_1^2}{z}\right)-e_2\frac{R_1^2}{z}\overline{F_P'}\left(\frac{R_1^2}{z}\right)\Bigg]$$
$$=w_3\Bigg[f_1\ln\frac{z-z_1}{z-z_2}+f_2T_N(z)+f_3H_P(z)-f_4zH_P'(z)$$
$$-f_5\overline{T_N}\left(\frac{R_2^2}{z}\right)+f_5\frac{R_2^2}{z}\overline{T_N'}\left(\frac{R_2^2}{z}\right)-f_5zT_P'(z)$$
$$-f_4\overline{H_N}\left(\frac{R_2^2}{z}\right)+f_4\frac{R_2^2}{z}\overline{H_N'}\left(\frac{R_2^2}{z}\right)-\frac{\tau_2^s}{R_2}\Bigg], \quad (43)$$
$$R_1^2\Bigg\{s_1F_N(z)+s_2zF_N'(z)+s_3\overline{T_P}\left(\frac{R_1^2}{z}\right)$$
$$+s_4\frac{R_1^2}{z}\overline{T_P'}\left(\frac{R_1^2}{z}\right)+s_5T_P(z)+s_6zT_N'(z)$$
$$+s_7\overline{F_P}\left(\frac{R_1^2}{z}\right)+s_8\frac{R_1^2}{z}\overline{F_P'}\left(\frac{R_1^2}{z}\right)-s_9z^{-2}+s_{10}\overline{F_N}\left(\frac{R_1^2}{z}\right)$$
$$-s_6T_N(z)-s_{11}-s_7z^2F_N''(z)-s_{12}z\left[\overline{T_P}\left(\frac{R_1^2}{z}\right)\right]'$$
$$+s_{12}R_1^2\left[\overline{T_P'}\left(\frac{R_1^2}{z}\right)\right]'-s_5zT_P'(z)-s_{12}z^2T_N''(z)$$
$$-s_7z\left[\overline{F_P}\left(\frac{R_1^2}{z}\right)\right]'+s_7R_1^2\left[\overline{F_P'}\left(\frac{R_1^2}{z}\right)\right]'$$
$$=R_2^2\Bigg\{t_1\ln\frac{z-z_1}{z-z_2}-t_2\frac{z}{z-z_1}+t_3\frac{z}{z-z_2}+t_4T_N(z)+t_5H_P(z)$$
$$+t_6zH_p'(z)+t_7\overline{T_N}\left(\frac{R_2^2}{z}\right)+t_8\frac{R_2^2}{z}\overline{T_N'}\left(\frac{R_2^2}{z}\right)-t_9zT_P'(z)$$
$$-t_{10}\overline{H_N}\left(\frac{R_2^2}{z}\right)+t_{11}\frac{R_2^2}{z}\overline{H_N'}\left(\frac{R_2^2}{z}\right)-t_{12}+t_{13}z$$
$$+t_{14}\overline{H_P}\left(\frac{R_2^2}{z}\right)+t_9T_P(z)-t_4zT_N'(z)+t_{10}z^2H_P''(z)$$
$$+t_{15}z\left[\overline{T_N}\left(\frac{R_2^2}{z}\right)\right]'-t_{15}R_2^2\left[\overline{T_N'}\left(\frac{R_2^2}{z}\right)\right]'+t_{15}z^2T_P''(z)$$
$$+t_{10}z\left[\overline{H_N}\left(\frac{R_2^2}{z}\right)\right]'-t_{10}R_2^2\left[\overline{H_N'}\left(\frac{R_2^2}{z}\right)\right]'\Bigg\}. \quad (44)$$

Equations (43) and (44) can be expanded in series by Laurent series expansion techniques, and the coefficients of the same power terms of z are compared. By solving these two equations, the unknown coefficients a_k, b_k, c_k, and d_k of Eqs. (43) and (44) can be obtained. Since the procedure leads to very cumbersome formulas for these coefficients, we do not show them here. The detailed expressions of the unknown coefficients are listed in the Appendix. According to Eqs. (11) and (12), two complex potentials $\Phi_1(z)$ and $\Psi_1(z)$ can be derived. The complex potentials $\Phi_2(z)$ and $\Psi_2(z)$ can be determined by Eqs. (32)–(34). Therefore, the complex potentials for the two material regions are obtained, and then the substitution of them into Eqs. (8)–(10) leads to the stress fields and the displacement fields in the NT and the matrix.

The detailed expressions of the complex potentials $\Phi_2(z)$ and $\Psi_2(z)$ are

$$\Phi_{20}(z)$$
$$=-\frac{1}{\kappa_2}\frac{D_2\omega}{2}\left(\ln\frac{z-z_2^*}{z-z_1^*}+\frac{z_1-z_1^*}{z-z_1^*}-\frac{z_2-z_2^*}{z-z_2^*}+\frac{z_2-z_1}{z}\right)$$
$$+\frac{\kappa_1\mu_2}{\kappa_2\mu_1}T_N(z)+\frac{\mu_2}{\kappa_2\mu_1}H_N(z), \quad (45)$$
$$\Psi_{20}(z)$$
$$=\frac{R_2^2}{z^2}\Bigg\{-\frac{1}{\kappa_2}\frac{D_2\omega}{2}\left(\ln\frac{z-z_2^*}{z-z_1^*}+\frac{z_1-z_1^*}{z-z_1^*}-\frac{z_2-z_2^*}{z-z_2^*}+\frac{z_2-z_1}{z}\right)$$
$$+\frac{1}{\kappa_2}\frac{D_2\omega}{2}\left[\frac{z}{z-z_2^*}-\frac{z}{z-z_1^*}-\frac{(z_1-z_1^*)z}{(z-z_1^*)^2}\right.$$
$$\left.+\frac{(z_2-z_2^*)z}{(z-z_2^*)^2}-\frac{z_2-z_1}{z}\right]$$
$$+\frac{D_2\omega}{2}\left[\ln\frac{z_1}{z_2}+\frac{(\overline{z_2}-\overline{z_1})}{R_2^2}z-\kappa_2\ln\frac{z-z_1^*}{z-z_2^*}-\kappa_2\ln\frac{\overline{z_1}}{\overline{z_2}}\right]$$
$$+\frac{D_2\omega}{2}\frac{z}{R_2^2}(\overline{z_1}-\overline{z_2})+\frac{\kappa_1\mu_2}{\kappa_2\mu_1}\left[T_N(z)-zT_N'(z)\right]$$
$$+\frac{\mu_2}{\kappa_2\mu_1}H_N(z)+\frac{\kappa_1\mu_2}{\mu_1}\overline{T_P}\left(\frac{R_2^2}{z}\right)$$
$$+\frac{\mu_2}{\mu_1}\overline{H_P}\left(\frac{R_2^2}{z}\right)-\frac{\mu_2}{\kappa_2\mu_1}zH_N'(z)\Bigg\}. \quad (46)$$

It is noticed that if the nanopore vanishes ($R_1\to 0$) our current model is reduced to a wedge disclination dipole near

a circular nanoinhomogeneity. Thus, equations (45) and (46) can be simplified as

$$\Phi_{20}(z) = -\frac{1}{\kappa_2}\frac{D_2\omega}{2}\left(\ln\frac{z-z_2^*}{z-z_1^*}+\frac{z_1-z_1^*}{z-z_1^*}-\frac{z_2-z_2^*}{z-z_2^*}+\frac{z_2-z_1}{z}\right) + \frac{\mu_2}{\kappa_2\mu_1}\left\{\overline{a_0}+\sum_{k=0}^{\infty}\left[(k-1)R_2^{2k}\overline{a_k}+R_2^{2k-2}\overline{c_k}\right]z^{-k}\right\}, \tag{47}$$

$$\begin{aligned}\Psi_{20}(z) = {} & \frac{R_2^2}{z^2}\left\{-\frac{1}{\kappa_2}\frac{D_2\omega}{2}\left(\ln\frac{z-z_2^*}{z-z_1^*}+\frac{z_1-z_1^*}{z-z_1^*}\right.\right. \\ & \left.-\frac{z_2-z_2^*}{z-z_2^*}+\frac{z_2-z_1}{z}\right) \\ & +\frac{1}{\kappa_2}\frac{D_2\omega}{2}\left[\frac{z}{z-z_2^*}-\frac{z}{z-z_1^*}-\frac{(z_1-z_1^*)z}{(z-z_1^*)^2}\right. \\ & \left.+\frac{(z_2-z_2^*)z}{(z-z_2^*)^2}-\frac{z_2-z_1}{z}\right] \\ & +\frac{D_2\omega}{2}\left[\ln\frac{z_1}{z_2}+\frac{(\overline{z_2}-\overline{z_1})}{R_2^2}z-\kappa_2\ln\frac{z-z_1^*}{z-z_2^*}-\kappa_2\ln\frac{\overline{z_1}}{\overline{z_2}}\right] \\ & +\frac{D_2\omega}{2}\frac{z}{R_2^2}(\overline{z_1}-\overline{z_2}) \\ & +\sum_{k=0}^{\infty}\left[\frac{\kappa_1\mu_2}{\mu_1}+\frac{\mu_2}{\kappa_2\mu_1}(k-1)(k+1)\right]R_2^{2k}\overline{a_k}z^{-k} \\ & +\sum_{k=0}^{\infty}\frac{\mu_2}{\kappa_2\mu_1}(k+1)R_2^{2k-2}\overline{c_k}z^{-k} \\ & \left.-\frac{\mu_2}{\mu_1}a_0+\frac{\mu_2}{\kappa_2\mu_1}\overline{a_0}\right\}, \end{aligned} \tag{48}$$

where

$$\begin{aligned} a_0 = {} & \left\{(\kappa_2+1)\frac{D_2\omega}{2}\left[(m_1-\alpha_2)\ln(z_1/z_2)+(\mu_2/\mu_1-1-\beta_2)\right.\right. \\ & \left.\times\ln(\overline{z_1}/\overline{z_2})\right]-(m_1-\alpha_2+\mu_2/\mu_1-1-\beta_2) \\ & \left.\times\alpha_2\tau_2^{\mathrm{s}}/R_2m_2\right\}\Big/\left[(m_1-\alpha_2)^2-(\mu_2/\mu_1-1-\beta_2)^2\right], \\ c_0 = {} & R\tau_2^{\mathrm{s}}/m_2, \\ a_1 = {} & \frac{D_2\omega}{2}\left\{(\kappa_2+1)\left(z_2^{-1}-z_1^{-1}\right)\right. \\ & -2\alpha_2\left(1+\frac{1}{\kappa_2}\right)/\left[R_2^2(m_2+\alpha_2)\right] \\ & \times\left[\overline{z_2}-\overline{z_1}+\overline{z_1^*}(1+\overline{z_1}\right. \\ & \left.\left.-\overline{z_1^*})-\overline{z_2^*}\left(1+\overline{z_2}-\overline{z_2^*}\right)\right]\right\}\Big/(m_1+\alpha_2+\beta_2), \\ c_1 = {} & \frac{D_2\omega}{2(m_2+\alpha_2)}\left(1+\frac{1}{\kappa_2}\right)\left[\overline{z_2}-\overline{z_1}+\overline{z_1^*}\left(1+\overline{z_1}-\overline{z_1^*}\right)\right. \\ & \left.-\overline{z_2^*}(1+\overline{z_2}-\overline{z_2^*})\right], \\ a_k = {} & \frac{D_2\omega}{2R_2^{2k}}\left\{(m_2+\alpha_2k)R_2^{2k}(\kappa_2+1)\left(z_2^{-k}-z_1^{-k}\right)/k\right. \\ & -\alpha_2(k+1)\left(1+\frac{1}{\kappa_2}\right)\left[\left(\overline{z_1^{*k}}-\overline{z_2^{*k}}\right)/k+\overline{z_1^{*k}}\left(\overline{z_1}-\overline{z_1^*}\right)\right. \\ & \left.\left.-\overline{z_2^{*k}}\left(\overline{z_2}-\overline{z_2^*}\right)\right]\right\}\Big/\left\{(m_2+\alpha_2k)\right. \\ & \times\left[m_1+\alpha_2\left(k^2+k-1\right)+k\beta_2\right]-\alpha_2(k+1) \\ & \left.\times\left[(m_2+\beta_2)(k-1)+\alpha_2\left(k^2-1\right)\right]\right\}, \quad (k\geq 2), \\ c_k = {} & \frac{D_2\omega}{2}\left\{\left[m_2(k+1)+\alpha_2\left(k^2-1\right)+\beta_2(k-1)\right]\right. \\ & \times R_2^{2k}(\kappa_2+1)\left(z_2^{-k}-z_1^{-k}\right)/k \\ & -\left[m_1+\alpha_2\left(k^2+k-1\right)+k\beta_2\right] \\ & \times\left(1+\frac{1}{\kappa_2}\right)\left[\left(\overline{z_1^{*k}}-\overline{z_2^{*k}}\right)/k+\overline{z_1^{*k}}\left(\overline{z_1}-\overline{z_1^*}\right)\right. \\ & \left.\left.-\overline{z_2^{*k}}\left(\overline{z_2}-\overline{z_2^*}\right)\right]\right\}\Big/\left\{\left[(m_2+\beta_2)(k-1)+\alpha_2\left(k^2-1\right)\right]\right. \\ & \times\alpha_2(k+1)R_2^{-2}-\left[m_1+\alpha_2\left(k^2+k-1\right)+k\beta_2\right] \\ & \left.\times(m_2+\alpha_2k)R_2^{2k-2}\right\}, \quad (k\geq 2), \\ m_1 = {} & \frac{\mu_2\kappa_1}{\mu_1}+1+\alpha_2+\beta_2, \quad m_2 = 1-\alpha_2+\frac{\mu_2}{\kappa_2\mu_1}. \end{aligned}$$

In order to validate the present reduced solution, the influence of the bulk material properties, such as shear modulus, on the force acting on the wedge disclination dipole center is examined without taking into account the interface effect, namely $R_1 = 0$, $\mu_1^{\mathrm{s}} = \mu_2^{\mathrm{s}} = 0$, $\lambda_1^{\mathrm{s}} = \lambda_2^{\mathrm{s}} = 0$, $\tau_1^{\mathrm{s}} = \tau_2^{\mathrm{s}} = 0$. In Fig. 2, let $\upsilon_1 = \upsilon_2 = 0.3$, $R_2 = 10$ nm, $p/R_2 = 0.1$ and $\varphi = \theta = 0$, then it will be easy to show that $f_y = 0$ in this case. Figure 2 indicates the variations of the normalized force $f_x/\mu_2\omega^2R_2$ with relative distance ρ/R_2 for different ratios of shear modulus μ_1/μ_2. We can see that the influence of the shear modulus on the force acting on the wedge disclination dipole center is in accordance with the results of Fig. 2 in the work of Luo and Liu.[54]

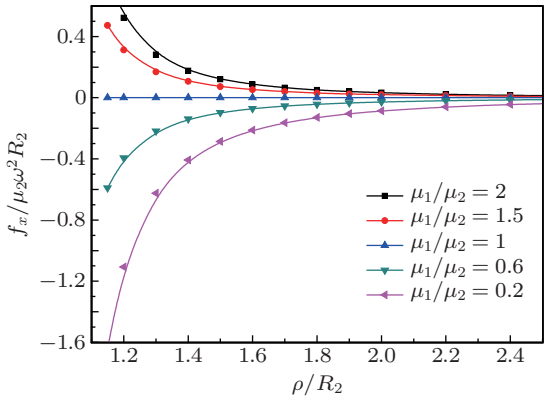


Fig. 2. (color online) Variations of $f_x/\mu_2\omega^2R_2$ with relative distance ρ/R_2 for $R_1 = 0$, $\mu_1^{\mathrm{s}} = \mu_2^{\mathrm{s}} = 0$, $\lambda_1^{\mathrm{s}} = \lambda_2^{\mathrm{s}} = 0$, $\tau_1^{\mathrm{s}} = \tau_2^{\mathrm{s}} = 0$, $\upsilon_1 = \upsilon_2 = 0.3$, $R_2 = 10$ nm, $p/R_2 = 0.1$, and $\varphi = \theta = 0$.

3. Force on disclination dipole

Following the Peach–Koehler formula, the perturbation force exerted on the wedge disclination dipole can be evalu-

ated. For ease of handling the influences of the various materials and geometric parameters on the perturbation force, we calculate approximately the perturbation force components per unit length on the center of the disclination dipole by the perturbation complex functions $\Phi_{20}(z_0)$, $\Psi_{20}(z_0)$, and $\Phi'_{20}(z_0)$, which are given by

$$f_x - \mathrm{i}f_y = 2\omega p \mathrm{e}^{\mathrm{i}\varphi}\left[\Phi_{20}(z_0) + \overline{\Phi_{20}(z_0)}\right] + 2\omega p \mathrm{e}^{-\mathrm{i}\varphi}\left[\overline{z_0}\Phi'_{20}(z_0) + \Psi_{20}(z_0)\right]. \quad (49)$$

With the aid of Eqs. (45) and (46), the perturbation force components f_x and f_y can be calculated.

4. Numerical studies

In the following sections, the influences of the NT and surface/interface stresses on the elastic behavior of the wedge disclination dipole are systematically discussed. In all the numerical studies, the forces exerted on the disclination dipole center are normalized as $f_{x0} = 4\pi f_x/\mu_2\omega^2 R_2$ and $f_{y0} = 4\pi f_y/\mu_2\omega^2 R_2$. Within the surface/interface elasticity used in the present work, the surface and interface are considered to be vanishingly thin layers which are characterized by their own surface/interface parameters: μ^{s}, λ^{s}, and τ^{s}. For the sake of definiteness, specifically we let $\mu_1^{\mathrm{s}} = \mu_2^{\mathrm{s}} = \mu_0^{\mathrm{s}}$, $\lambda_1^{\mathrm{s}} = \lambda_2^{\mathrm{s}} = \lambda_0^{\mathrm{s}}$. Therefore, we can introduce the following elastic intrinsic lengths $a = \mu_0^{\mathrm{s}}/\mu_2$, $b = \lambda_0^{\mathrm{s}}/\mu_2$, $c = \tau_1^{\mathrm{s}}/\mu_2$, and $d = \tau_2^{\mathrm{s}}/\mu_2$. Note that the elastic intrinsic lengths a, b, c, and d have the dimension of length. Previous studies have shown that a, b, c, and d are of the order of 0.1 nm and their values can be positive or negative, depending on the crystallographic orientation.[67] In addition, the following physical quantities can be normalized: the ratio between the shear modulus of the NT layer and the matrix as $\alpha = \mu_1/\mu_2$, the relative thickness of the NT layer as $\lambda = R_2/R_1$, the relative value of the disclination dipole center to the outer radius of the NT layer as $\delta = \rho/R_2$, which characterizes the relative distance of the dipole center to the interface of the NT, and the semi length of dipole arm relative to the NT layer as $\chi = p/R_2$. Without loss of generality, the wedge disclination dipole is assumed to lie on the x axis, i.e., $\varphi = \theta = 0$ unless otherwise stated. In this case f_{y0} is zero due to the symmetry of the problem.

The curves in Fig. 3 show the effects of the shear modulus mismatch of the NT layer and matrix on the force acting on the center of the wedge disclination dipole without surface/interface effects. When $a = b = c = d = 0$, the surface/interface effects of the NT are ignored and the composite material becomes a traditional two-phase composite material. We can see that as the wedge disclination dipole is located closer to the outer interface from the matrix, the repulsive or attractive force of the NT, exerted on the disclination dipole, becomes sharper. When the coating layer is much softer than the matrix, the disclination dipole is always attracted by the coating layer and has no equilibrium position in the case under consideration. When the coating layer is harder than the matrix, the disclination dipole might be first attracted and then repelled, being kept away from the composites. An unstable equilibrium position of the wedge disclination dipole can be found at about $\delta = 1.7$ near the hard coating layer for $\alpha = 1.2$. When the coating layer is sufficiently harder than the matrix, the disclination dipole is repelled all the time.

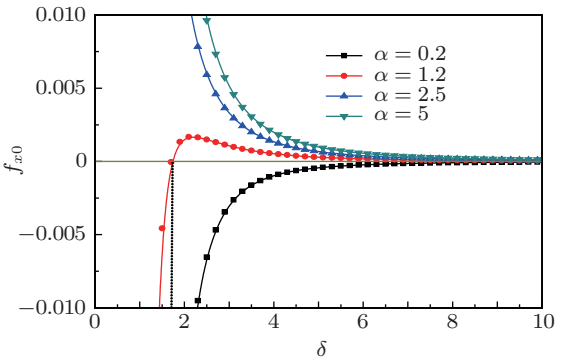


Fig. 3. (color online) Dependences of normalized force f_{x0} on the relative center position of the disclination dipole δ for $a = b = c = d = 0$, $\lambda = 1.5$, $\chi = 0.006$, $R_1 = 100$ nm, $\varphi = \theta = 0$, $\upsilon_1 = 0.1$, and $\upsilon_2 = 0.3$.

In Fig. 4, we show the variations of the normalized force f_{x0} with the ratio between the shear modulus of NT and matrix α for different surface/interface stresses. It clearly indicates that as the NT layer hardens, the attractive force on the disclination dipole sharply reduces and then turns into a repulsive force. There exists a critical ratio of the shear modulus α_{c} to keep the dipole center in equilibrium. For instance, the critical ratio $\alpha_{\mathrm{c}} = 1.85$ for $a = b = c = d = 0$. Within the nonclassical approach, the surface/interface causes different effects on the force exerted on the disclination dipole, depending on the positive or negative values of the surface/interface elastic constants and residual surface/interface tensions. It is seen that the surface/interface characterized by the positive surface/interface elastic constants or the negative residual surface/interface tensions contributes to the repulsive force of the NT on the disclination dipole. In addition, the positive surface/interface elastic constants and the negative residual surface/interface tensions reduce the critical ratio of the shear modulus to keep the dipole center in equilibrium. In other words, the NT needs to be harder to keep the dipole center in equilibrium with the surface/interface characterized by the negative surface/interface elastic constants or the positive residual surface/interface tensions.

From the above two figures, we observe that the shear modulus and the surface/interface stresses of the NT can change not only the location of the equilibrium position, but also the stability of the disclination dipole.

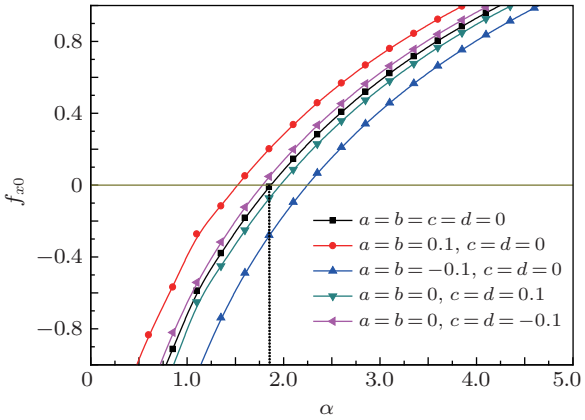


Fig. 4. (color online) Dependences of normalized force f_{x0} on the ratio of the shear modulus of the NT and matrix α for $\lambda = 1.1$, $\chi = 0.05$, $\delta = 1.05$, $R_1 = 10$ nm, $\varphi = \theta = 0$, $\upsilon_1 = 0.1$, and $\upsilon_2 = 0.3$.

Figure 5 shows the variations of f_{x0} with δ for different Poisson ratios and surface/interface elastic constants with $\lambda = 1.1$, $\chi = 0.05$, $\alpha = 1.2$, $R_1 = 10$ nm, $\varphi = \theta = 0$, and $\upsilon_2 = 0.2$. It is noted that the influence of Poisson ratio mismatch increases dramatically as the wedge disclination dipole approaches the NT. It also indicates that increasing the Poisson ratio of the NT layer impedes the attraction and contributes to the repulsion of the NT on the disclination dipole. Thus, the unstable equilibrium position is close to the outer interface of the NT with the increase of the Poisson ratio of the NT layer. Moreover, it is seen that the surface/interface of the NT with positive (negative) surface/interface elastic constants adds an extra repulsive (attractive) force to the force obtained within the classical elasticity. This additional force becomes stronger when the disclination dipole moves toward the NT and finally tends to infinity when it reaches the outer interface of the NT. From this figure, we conclude that the Poisson ratio and the surface/interface stresses of the NT layer have a significant effect on the force and the equilibrium location of the disclination dipole.

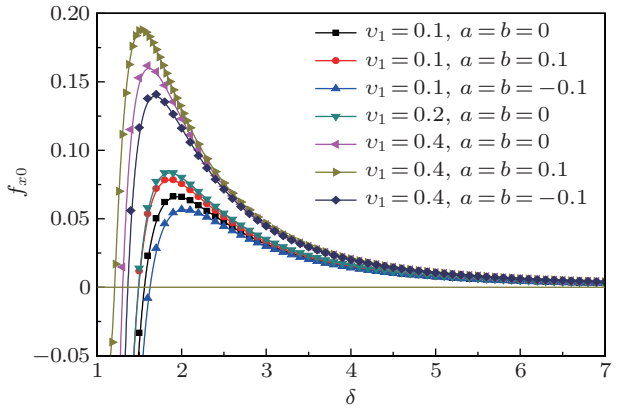


Fig. 5. (color online) Dependences of normalized force f_{x0} on the relative center position of the disclination dipole δ for $\lambda = 1.1$, $\chi = 0.05$, $\alpha = 1.2$, $R_1 = 10$ nm, $\varphi = \theta = 0$, and $\upsilon_2 = 0.2$.

For $a = b = 0$, $\chi = 0.05$, $\delta = 1.05$, $\varphi = \theta = 0$, $\upsilon_1 = \upsilon_2 = 0.2$ and $R_1 = 15$ nm, figure 6 demonstrates the variations of f_{x0} with the thickness of the NT layer with different ratios of the shear modulus and the residual surface/interface tensions. It is clear from the figure that when the NT layer is relatively thin, the attraction is increasingly weakened and the repulsion is rapidly strengthened with the thickening of the NT due to the harder NT layer. In this case, the positive (negative) residual surface/interface tensions contribute to the attractive (repulsive) force acting on the disclination dipole. Moreover, the surface/interface stresses have relatively less effect on the force acting on the disclination dipole. However, when the thickness of the NT layer is large enough, the effect of the thickness of the NT layer on the repulsive or attractive force is correspondingly mild. Interestingly, as the NT layer thickens, the surface/interface effect becomes considerable, while the surface/interface stresses characterized by negative residual surface/interface tensions cause an extra force which increases the attraction or reduces the repulsion of the NT to the disclination dipole. These results have not been found in previous studies.

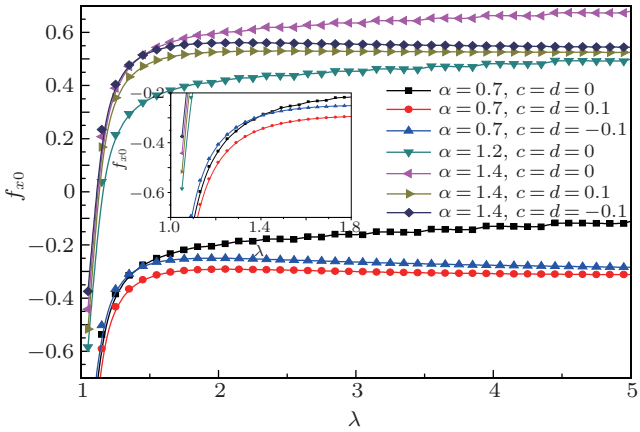


Fig. 6. (color online) Dependences of normalized force f_{x0} on the relative thickness of the NT layer λ for $R_1 = 15$ nm, $\chi = 0.05$, $\delta = 1.05$, $\varphi = \theta = 0$, $\upsilon_1 = \upsilon_2 = 0.2$, and $a = b = 0$. Inset is an enlarged figure with λ ranging from 1.0 to 1.8.

The variations of the normalized force f_{x0} with a relative center position of the disclination dipole δ are depicted in Fig. 7 for different values of disclination strength ω. As can be seen in the figure, when the NT layer is harder than the matrix, and the Poisson ratio of the NT layer is the same as that of the matrix, the disclination dipole is first attracted and then repelled by the NT as the disclination dipole goes away from the NT–matrix interface. The repulsive force first sharply increases and then slowly decreases as the disclination dipole is kept away from the interface, leading to the maximum value of the repulsive force. Enhancement of the disclination strength ω results in the increment of the attractive or repulsive force, and the maximum value of the repulsive force acting on the disclination dipole in such a situation. However, when the

disclination dipole goes far enough, i.e. $\delta = 7$, the effect of the disclination strength is negligibly small.

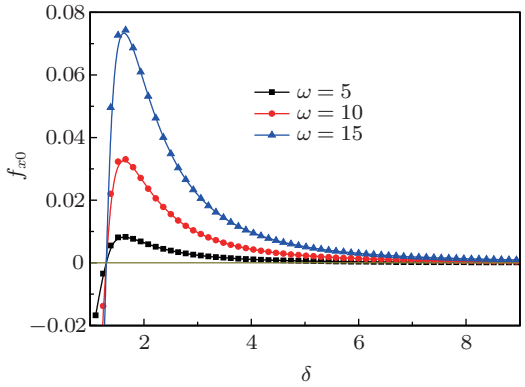


Fig. 7. (color online) Dependences of normalized force f_{x0} on the relative center position of the disclination dipole δ for $a = b = c = d = 0$, $\alpha = 1.2$, $R_1 = 15$ nm, $\chi = 0.05$, $\lambda = 1.2$, $\varphi = \theta = 0$, and $\upsilon_1 = \upsilon_2 = 0.2$.

Suppose that the disclination dipole is located at the arbitrary position in the matrix, then the force f_{y0} will not be zero in this case. Therefore, the dependences of the normalized forces f_{x0} and f_{y0} on the relative center position of the disclination dipole δ for different wedge disclination angles φ and dipole location angles θ are plotted in Figs. 8(a) and 8(b) for $\alpha = 1.2$, $\lambda = 1.2$, $R_1 = 15$ nm, $\chi = 0.05$, $\upsilon_1 = \upsilon_2 = 0.2$, and $a = b = c = d = 0$. We can see that without the surface/interface effects, one can obtain quite different forces f_{x0} and f_{y0} acting on the disclination dipole due to the NT, intensively depending on the wedge disclination angle φ and dipole location angle θ, especially when the disclination dipole is very close to the NT. For the force component f_{x0}, as shown in Fig. 8(a), the disclination dipole is first attracted and then repelled as the disclination dipole is far away from the NT–matrix interface. As the wedge disclination angle φ and dipole location angle θ increase in a range of 0°–90°, the repulsive force decays, and then changes into an attractive force. Therefore the unstable equilibrium position may disappear, and even turn into the stable one. For example, it has no equilibrium position for $\varphi = \theta = 30°$, while a stable equilibrium position can be found for $\varphi = \theta = 45°$. The force f_{x0} is always zero when $\varphi = \theta = 90°$. However, when the disclination dipole crosses the position $\phi = \theta = 90°$ to a region of 90°–180°, the NT may again first attract and then repel the disclination dipole, causing an unstable equilibrium position. It is also noted in Fig. 8(b), the similar influences of the wedge disclination angle φ and dipole location angle θ on the force f_{y0} are found except for some special conditions. For example, the force f_{y0} is still always zero when $\varphi = \theta = 0°$. Besides, when $\varphi = \theta = 90°$, the disclination dipole is subjected to the strongest attractive or repulsive force exerted by the NT and has a stable equilibrium position around $\delta = 1.3$.

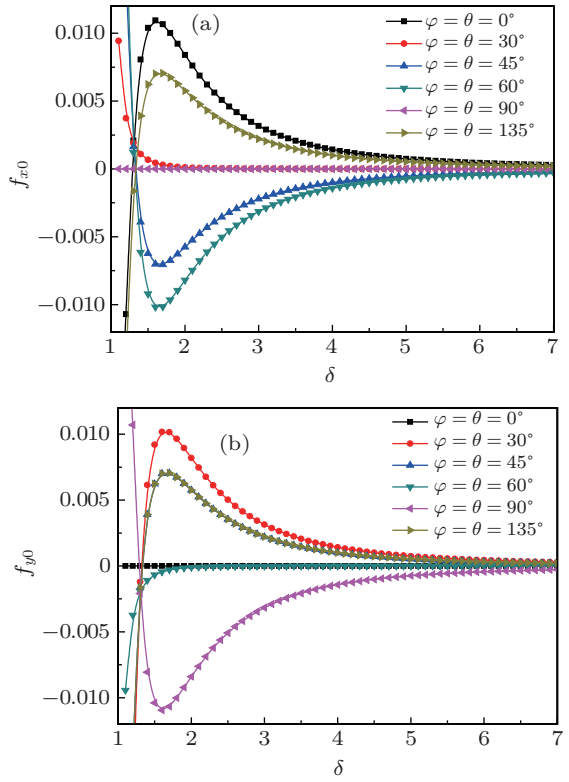


Fig. 8. (color online) Dependences of normalized forces f_{x0} (a) and f_{y0} (b) on the relative center position of the disclination dipole δ for $\alpha = 1.2$, $\lambda = 1.2$, $R_1 = 15$ nm, $\chi = 0.05$, $\upsilon_1 = \upsilon_2 = 0.2$, and $a = b = c = d = 0$.

In Fig. 9, in order to conveniently analyze the results, we assume again that the center of the wedge disclination dipole is located on the x axis. The following demonstrations are the variations of the normalized forces f_{x0} and f_{y0} with wedge disclination angle φ for different thickness values of the NT layer and surface/interface stresses when the disclination dipole moves along the x axis (Fig. 9). Figures 9(a) and 9(b) show the effects of the thickness of the NT layer and the surface/interface elastic constants on the normalized forces f_{x0} and f_{y0} for $\alpha = 1.2$, $R_1 = 15$ nm, $\delta = 1.05$, $\chi = 0.05$, $\upsilon_1 = \upsilon_2 = 0.2$, $\theta = 0$, and $c = d = 0$. As we can see, the normalized forces f_{x0} and f_{y0} are still an even and an odd function of the wedge disclination angle φ, respectively. As the thickness of the NT layer increases, the NT has a relatively major role in the force acting on the disclination dipole in the NT-based composites. That is, when the NT layer becomes thick enough, the nanopore is less influential in the disclination dipole. If the thickness of the NT is large enough, the equilibrium position will emerge in this case. For the normalized force f_{x0} in Fig. 9(a), the surface/interface effects characterized by the positive surface/interface elastic constants reduce the attractive force and increase the repulsion in some ranges. For $\lambda = 1.1$, the range is about $0° \le \varphi \le 60°$ and $120° \le \varphi \le 180°$, and for $\lambda = 1.3$, $0° \le \varphi \le 70°$ and $110° \le \varphi \le 180°$. However, in a range of $60° \le \varphi \le 120°$ for $\lambda = 1.1$, the surface/interface stresses show the inverse in-

fluence on the normalized force f_{x0}. As shown in Fig. 9(b), the surface/interface effects characterized by the positive (negative) surface/interface elastic constants reduce (enlarge) the attractive force in a range of $0 \leq \varphi \leq 90°$. However, the surface/interface stresses show the inverse influence on the normalized force f_{y0} in a range of $90° \leq \varphi \leq 180°$. In addition, note that the force always equals zero at the points $\varphi = 0°$, 90°, and 180°. From these two figures, we can see that the equilibrium position may occur, even more than one, owing to the influence of the surface/interface stresses and the increase of the NT layer thickness. Furthermore, the cooperative influences of the surface/interface stresses and the thickness of the NT layer on the force are greatly dependent on the disclination angle φ.

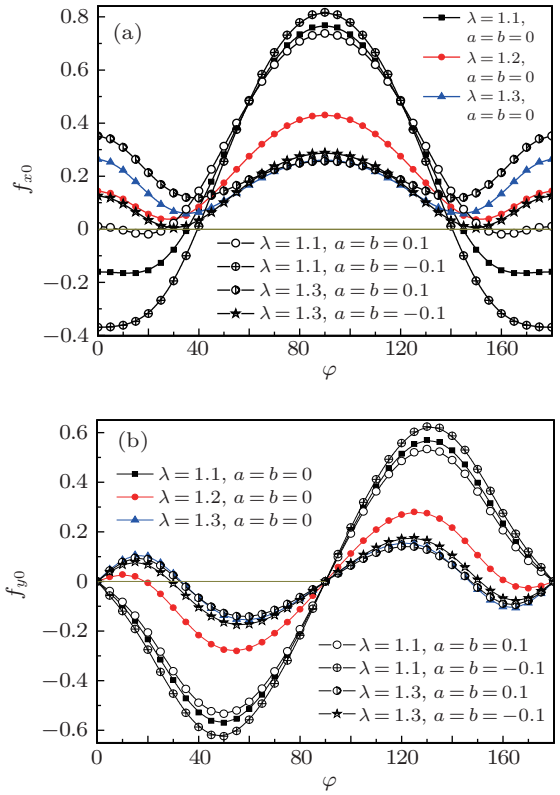


Fig. 9. (color online) Dependences of the normalized forces f_{x0} (a) and f_{y0} (b) on disclination angle φ for $\alpha = 1.2$, $R_1 = 15$ nm, $\delta = 1.05$, $\chi = 0.05$, $\upsilon_1 = \upsilon_2 = 0.2$, $\theta = 0$, and $c = d = 0$.

5. Conclusions

The elastic behavior of a wedge disclination dipole located in NT-based composites is studied within the framework of surface/interface elasticity theory. The explicit expression for the force acting on the wedge disclination dipole is obtained by means of a complex variable method. The influences of material elastic dissimilarity, the NT thickness and the features of the disclination dipole, and surface/interface effect on the force are evaluated. Some conclusions drawn from the present study are summarized as follows.

i) The influence of the material elastic dissimilarity on the force increases dramatically as the wedge disclination dipole approaches the NT. When the NT is much softer than the matrix, the disclination dipole is always attracted by the NT and has no equilibrium position. When the NT is harder than the matrix, the disclination dipole might be first attracted and then repelled, being kept away from the NT, leading to an unstable equilibrium position of the disclination dipole. There exists a critical ratio of the shear modulus to keep the dipole center in equilibrium. When the NT is sufficiently harder than the matrix, the disinclination dipole is repelled all the time. Increasing the Poisson ratio of the NT layer impedes the attraction and contributes to the repulsion of the NT on the disclination dipole.

ii) When the NT is relatively thin, the attraction is increasingly weakened and the repulsion is rapidly strengthened with the thickening of the NT due to harder NT layer. However, as the thickness of the NT layer increases, the NT has a relatively major role in the force acting on the disclination dipole in the NT-based composites.

iii) The enhancement of the disclination strength results in the increment of the attractive or repulsive force on the disclination dipole. However, when disclination dipole goes far enough away from the NT, the effect of the disclination strength is negligibly small. Due to the effect of the hard NT, as the wedge disclination angle and dipole location angle increase in the range of 0°–90°, the repulsive force decays, and then changes into an attractive force, which makes the unstable equilibrium position disappear, even a stable one may occur.

iv) The positive surface/interface elastic constants and the negative residual surface/interface tensions reduce the critical ratio of the shear modulus to keep the dipole center in equilibrium. As the NT layer thickens, the surface/interface effect becomes considerable. The equilibrium position may occur, even more than one, owing to the influences of the surface/interface stresses and NT thickening. The influences of the surface/interface stresses and the thickness of the NT layer on the force are greatly dependent on the disclination angle.

Appendix A

$$a_0 = \frac{(y_{02}y_{09} - y_{03}y_{08})(y_{06}v_{01} - y_{03}v_{02}) - (y_{02}y_{06} - y_{03}y_{05})(y_{09}v_{01} - y_{03}v_{03})}{(y_{01}y_{06} - y_{03}y_{04})(y_{02}y_{09} - y_{03}y_{08}) - (y_{02}y_{06} - y_{03}y_{05})(y_{01}y_{09} - y_{03}y_{07})},$$

$$c_0 = \frac{(y_{01}y_{09} - y_{03}y_{07})(y_{06}v_{01} - y_{03}v_{02}) - (y_{01}y_{06} - y_{03}y_{04})(y_{09}v_{01} - y_{03}v_{03})}{(y_{02}y_{06} - y_{03}y_{05})(y_{01}y_{09} - y_{03}y_{07}) - (y_{01}y_{06} - y_{03}y_{04})(y_{02}y_{09} - y_{03}y_{08})},$$

$$y_{01}=x_{01}x_{06}-x_{02}x_{05},\quad y_{02}=x_{03}x_{06}-x_{02}x_{07},$$
$$y_{03}=x_{04}x_{06}-x_{02}x_{08},\quad y_{04}=x_{01}x_{09}-x_{02}x_{010},$$
$$y_{05}=x_{03}x_{09}+x_{02}x_{012},\quad y_{06}=x_{04}x_{09}+x_{02}x_{011},$$
$$y_{07}=x_{01}x_{013}-x_{02}x_{014},\quad y_{08}=x_{03}x_{013}+x_{02}x_{016},$$
$$y_{09}=x_{04}x_{013}+x_{02}x_{015},\quad v_{01}=x_{06}u_{01}-x_{02}u_{02},$$
$$v_{02}=x_{09}u_{01}-x_{02}u_{03},\quad v_{03}=x_{013}u_{01}-x_{02}u_{04},$$
$$x_{01}=w_1\left(e_4-e_2\right),\quad x_{02}=w_1e_3+w_3f_3,\quad x_{03}=w_1e_2,$$
$$x_{04}=w_3f_3,\quad x_{05}=R_1^2\left(s_5-s_7\right)+R_2^2\left(t_{14}-t_9\right),$$
$$x_{06}=R_1^2s_3+R_2^2t_5,\quad x_{07}=s_7-t_{14},\quad x_{08}=t_5,$$
$$x_{09}=\overline{x_{01}},\quad x_{010}=\overline{x_{02}},\quad x_{011}=\overline{x_{03}},$$
$$x_{012}=\overline{x_{04}},\quad x_{013}=\overline{x_{05}},\quad x_{014}=\overline{x_{06}},\quad x_{015}=\overline{x_{07}},$$
$$x_{016}=\overline{x_{08}},\quad u_{01}=w_3f_1\ln\left(z_1/z_2\right)-w_3\tau_2^{\mathrm{s}}/R_2,$$
$$u_{02}=R_2^2\left(t_1+w_4f_6\right)\ln\left(z_1/z_2\right)+R_1^2s_{12}-R_2^2t_{12},$$
$$u_{03}=\overline{u_{01}},\quad u_{04}=\overline{u_{02}},\quad a_1=\frac{x_{124}v_{11}-x_{14}v_{12}}{x_{11}x_{124}-x_{14}x_{121}},$$
$$b_1=y_{13},\quad c_1=y_{12},\quad d_1=\frac{x_{113}v_{13}-x_{19}v_{14}}{x_{112}x_{113}-x_{19}x_{116}},$$
$$v_{11}=u_{11}-x_{12}y_{11}-x_{13}y_{12},\quad v_{12}=-x_{122}y_{11}-x_{123}y_{12},$$
$$v_{13}=-x_{110}y_{13}-x_{115}y_{14},\quad v_{14}=u_{13}-x_{114}y_{13}-x_{115}y_{14},$$
$$y_{11}=\frac{x_{120}u_{12}}{x_{15}x_{120}-x_{16}x_{119}},\quad y_{12}=\frac{x_{119}u_{12}}{x_{16}x_{119}-x_{15}x_{120}},$$
$$y_{13}=\frac{x_{18}u_{14}}{x_{18}x_{117}-x_{17}x_{118}},\quad y_{14}=\frac{x_{17}u_{14}}{x_{17}x_{118}-x_{18}x_{117}},$$
$$x_{11}=w_1e_4,\quad x_{12}=2w_3\left(f_3-f_4+f_5\right)R_2^{-2},$$
$$x_{13}=2w_3f_4R_2^{-2},\quad x_{14}=w_3\left(f_4-f_3\right),$$
$$x_{15}=2t_5+2t_6-t_7+t_8-3t_{15},$$
$$x_{16}=s_9-2t_{10}+t_{11},\quad x_{17}=-w_1e_3-w_3f_2,$$
$$x_{18}=w_1e_1-w_1e_2,\quad x_{19}=s_3+s_4+s_{11},$$
$$x_{110}=R_1^2\left(-2s_8-2s_6-2s_{11}-4s_7\right)+R_2^2\left(-2t_4+2t_{14}\right),$$
$$x_{111}=s_1-s_2-2s_7,\quad x_{112}=s_8+2s_7-t_{14},$$
$$x_{113}=\overline{x_{11}},\quad x_{114}=\overline{x_{12}},\quad x_{115}=\overline{x_{13}},$$
$$x_{116}=\overline{x_{14}},\quad x_{117}=\overline{x_{15}},\quad x_{118}=\overline{x_{16}},$$
$$x_{119}=\overline{x_{17}},\quad x_{120}=\overline{x_{18}},\quad x_{121}=\overline{x_{19}},$$
$$x_{122}=\overline{x_{110}},\quad x_{123}=\overline{x_{111}},\quad x_{124}=\overline{x_{112}},$$
$$u_{11}=w_3f_1\left(z_2^{-1}-z_1^{-1}\right),$$
$$u_{12}=R_2^2\left(-t_1z_1^{-1}+t_1z_2^{-1}+t_2z_1^{-1}-t_3z_2^{-1}+t_{13}\right),$$
$$u_{13}=\overline{u_{11}},\quad u_{14}=\overline{u_{12}},$$

$$a_2=\frac{\left(y_{22}y_{29}-y_{23}y_{28}\right)\left(y_{26}v_{21}-y_{23}v_{22}\right)-\left(y_{22}y_{26}-y_{23}y_{25}\right)\left(y_{29}v_{21}-y_{23}v_{23}\right)}{\left(y_{21}y_{26}-y_{23}y_{24}\right)\left(y_{22}y_{29}-y_{23}y_{28}\right)-\left(y_{21}y_{29}-y_{23}y_{27}\right)\left(y_{22}y_{26}-y_{23}y_{25}\right)},$$
$$b_2=\frac{\left(y_{212}y_{217}-y_{211}y_{218}\right)\left(y_{214}v_{24}-y_{211}v_{25}\right)-\left(y_{212}y_{214}-y_{211}y_{215}\right)\left(y_{217}v_{24}-y_{211}v_{26}\right)}{\left(y_{210}y_{214}-y_{211}y_{213}\right)\left(y_{212}y_{217}-y_{211}y_{218}\right)-\left(y_{210}y_{217}-y_{211}y_{216}\right)\left(y_{212}y_{214}-y_{211}y_{215}\right)},$$
$$c_2=\frac{\left(y_{21}y_{29}-y_{23}y_{27}\right)\left(y_{26}v_{21}-y_{23}v_{22}\right)-\left(y_{21}y_{26}-y_{23}y_{24}\right)\left(y_{29}v_{21}-y_{23}v_{23}\right)}{\left(y_{21}y_{29}-y_{23}y_{27}\right)\left(y_{22}y_{26}-y_{23}y_{25}\right)-\left(y_{21}y_{26}-y_{23}y_{24}\right)\left(y_{22}y_{29}-y_{23}y_{28}\right)},$$
$$d_2=\frac{\left(y_{210}y_{217}-y_{211}y_{216}\right)\left(y_{214}v_{24}-y_{211}v_{25}\right)-\left(y_{210}y_{214}-y_{211}y_{213}\right)\left(y_{217}v_{24}-y_{211}v_{26}\right)}{\left(y_{210}y_{214}-y_{211}y_{213}\right)\left(y_{212}y_{217}-y_{211}y_{218}\right)-\left(y_{210}y_{217}-y_{211}y_{216}\right)\left(y_{212}y_{214}-y_{211}y_{215}\right)},$$

$$y_{21}=x_{21}x_{26}-x_{22}x_{25},\quad y_{22}=x_{23}x_{26}-x_{22}x_{27},$$
$$y_{23}=x_{24}x_{26}+x_{22}x_{28},\quad y_{24}=x_{21}x_{226}-x_{22}x_{225},$$
$$y_{25}=x_{23}x_{226}-x_{22}x_{227},\quad y_{26}=x_{24}x_{226}+x_{22}x_{228},$$
$$y_{27}=x_{21}x_{230}-x_{22}x_{229},\quad y_{28}=x_{23}x_{230}-x_{22}x_{231},$$
$$y_{29}=x_{24}x_{230}-x_{22}x_{232},\quad y_{210}=x_{210}x_{213}-x_{29}x_{214},$$
$$y_{211}=x_{211}x_{213}-x_{29}x_{215},\quad y_{212}=x_{212}x_{213}+x_{29}x_{216},$$
$$y_{213}=x_{210}x_{217}-x_{29}x_{218},\quad y_{214}=x_{211}x_{217}-x_{29}x_{219},$$
$$y_{215}=x_{212}x_{217}+x_{29}x_{220},\quad y_{216}=x_{210}x_{221}-x_{29}x_{222},$$
$$y_{217}=x_{211}x_{221}-x_{29}x_{223},\quad y_{218}=x_{212}x_{221}-x_{29}x_{224},$$
$$v_{21}=x_{26}u_{21}-x_{22}u_{22},\quad v_{22}=x_{226}u_{21}-x_{22}u_{27},$$
$$v_{23}=x_{230}u_{21}-x_{22}u_{28},\quad v_{24}=x_{213}u_{23}-x_{29}u_{24},$$
$$v_{25}=x_{217}u_{23}-x_{29}u_{25},\quad v_{26}=x_{221}u_{23}-x_{29}u_{26},$$
$$x_{21}=w_1e_4+2w_3f_5+3w_3f_4,$$
$$x_{22}=3w_3f_3-6w_3f_4+3w_3f_5,$$
$$x_{23}=3w_3f_4R_2^{-2},\quad x_{24}=\left(2f_4-f_3\right)w_3R_2^{-6},$$
$$x_{25}=R_1^2\left(s_9-s_5\right)+R_2^2\left(t_9+2t_{11}-2t_{15}-7t_{10}\right),$$
$$x_{26}=\left(3t_5+6t_6-t_7+2t_8+6t_{10}-8t_{15}\right)R_2^{-2},$$
$$x_{27}=s_9-7t_{10}+2t_{11},\quad x_{28}=t_5+2t_6+2t_{10},$$
$$x_{29}=\left(e_1-2e_2-e_3\right)w_1R_1^4,\quad x_{210}=3w_1e_2-2w_1e_3-w_3f_2,$$
$$x_{211}=\left(e_1-2e_2\right)w_1R_1^2,\quad x_{212}=w_1e_2R_1^{-2},$$
$$x_{213}=\left(s_1-2s_2+s_3+2s_4-6s_7\right)R_1^6,$$
$$x_{214}=R_1^2\left(-6s_8-3s_6-6s_{11}-3s_7\right)+R_2^2\left(3t_{14}-3t_4\right),$$
$$x_{215}=\left(s_1-2s_2-6s_7\right)R_1^4,\quad x_{216}=2s_8+s_7-t_{14},$$
$$x_{217}=\overline{x_{21}},\quad x_{218}=\overline{x_{22}},\quad x_{219}=\overline{x_{23}},\quad x_{220}=\overline{x_{24}},$$
$$x_{221}=\overline{x_{25}},\quad x_{222}=\overline{x_{26}},\quad x_{223}=\overline{x_{27}},\quad x_{224}=\overline{x_{28}},$$
$$x_{225}=\overline{x_{29}},\quad x_{226}=\overline{x_{210}},\quad x_{227}=\overline{x_{211}},\quad x_{228}=\overline{x_{212}},$$
$$x_{229}=\overline{x_{213}},\quad x_{230}=\overline{x_{214}},\quad x_{231}=\overline{x_{215}},\quad x_{232}=\overline{x_{216}},$$
$$u_{21}=0.5w_3f_1\left(z_2^{-2}-z_1^{-2}\right),$$
$$u_{22}=R_2^2\left(0.5t_1z_2^{-2}-0.5t_1z_1^{-2}+t_2z_1^{-2}-t_3z_2^{-2}\right),$$
$$u_{23}=0,\quad u_{24}=R_1^2s_9,\quad u_{25}=\overline{u_{21}},$$
$$u_{26}=\overline{u_{22}},\quad u_{27}=\overline{u_{23}},\quad u_{28}=\overline{u_{24}},$$

$$a_k = \frac{(y_{k2}y_{k9}-y_{k3}y_{k8})(y_{k6}v_{k1}-y_{k3}v_{k2})-(y_{k2}y_{k6}-y_{k3}y_{k5})(y_{k9}v_{k1}-y_{k3}v_{k3})}{(y_{k1}y_{k6}-y_{k3}y_{k4})(y_{k2}y_{k9}-y_{k3}y_{k8})-(y_{k1}y_{k9}-y_{k3}y_{k7})(y_{k2}y_{k6}-y_{k3}y_{k5})},$$

$$b_k = \frac{(y_{k11}y_{k18}+y_{k12}y_{k17})y_{k11}v_{k4}+(y_{k11}y_{k15}-y_{k12}y_{k14})y_{k11}v_{k5}}{(y_{k11}y_{k13}-y_{k10}y_{k14})(y_{k11}y_{k18}+y_{k12}y_{k17})-(y_{k11}y_{k16}-y_{k10}y_{k17})(y_{k11}y_{k15}-y_{k12}y_{k14})},$$

$$c_k = \frac{(y_{k1}y_{k9}-y_{k3}y_{k7})(y_{k6}v_{k1}-y_{k3}v_{k2})-(y_{k1}y_{k6}-y_{k3}y_{k4})(y_{k9}v_{k1}-y_{k3}v_{k3})}{(y_{k1}y_{k9}-y_{k3}y_{k7})(y_{k2}y_{k6}-y_{k3}y_{k5})-(y_{k1}y_{k6}-y_{k3}y_{k4})(y_{k2}y_{k9}-y_{k3}y_{k8})},$$

$$d_k = \frac{(y_{k11}y_{k16}-y_{k10}y_{k17})y_{k11}v_{k4}-(y_{k11}y_{k13}-y_{k10}y_{k14})y_{k11}v_{k5}}{(y_{k11}y_{k16}-y_{k10}y_{k17})(y_{k11}y_{k15}-y_{k12}y_{k14})-(y_{k11}y_{k13}-y_{k10}y_{k14})(y_{k11}y_{k18}+y_{k12}y_{k17})}, \quad (k\geq 3),$$

$$y_{k1}=x_{k1}x_{k6}-x_{k2}x_{k5}, \quad y_{k2}=x_{k2}x_{k6}-x_{k2}x_{k7},$$

$$y_{k3}=x_{k4}x_{k6}+x_{k2}x_{k8}, \quad y_{k4}=x_{k1}x_{k26}-x_{k2}x_{k25},$$

$$y_{k5}=x_{k3}x_{k26}-x_{k2}x_{k27}, \quad y_{k6}=x_{k4}x_{k26}-x_{k2}x_{k28},$$

$$y_{k7}=x_{k1}x_{k30}-x_{k2}x_{k29}, \quad y_{k8}=x_{k3}x_{k30}-x_{k2}x_{k31},$$

$$y_{k9}=x_{k4}x_{k30}-x_{k2}x_{k32}, \quad y_{k10}=x_{k10}x_{k13}-x_{k9}x_{k14},$$

$$y_{k11}=x_{k11}x_{k13}-x_{k9}x_{k15}, \quad y_{k12}=x_{k12}x_{k13}-x_{k9}x_{k16},$$

$$y_{k13}=x_{k9}x_{k18}-x_{k10}x_{k17}, \quad y_{k14}=x_{k9}x_{k19}-x_{k11}x_{k17},$$

$$y_{k15}=x_{k9}x_{k20}-x_{k12}x_{k17}, \quad y_{k16}=x_{k9}x_{k22}-x_{k10}x_{k21},$$

$$y_{k17}=x_{k9}x_{k23}-x_{k11}x_{k21}, \quad y_{k18}=x_{k9}x_{k24}+x_{k12}x_{k21},$$

$$v_{k1}=x_{k6}u_{k1}-x_{k2}u_{k2}, \quad v_{k2}=x_{k26}u_{k1},$$

$$v_{k3}=x_{k30}u_{k1}, \quad v_{k4}=x_{k9}u_{k3}, \quad v_{k5}=x_{k9}u_{k4},$$

$$x_{k1}=w_1e_4+kw_3f_5+(k-1)(k+1)w_3f_4,$$

$$x_{k2}=(f_3-kf_4+f_5)(k+1)w_3R_2^{-2k},$$

$$x_{k3}=(k+1)w_3f_4R_2^{-2}, \quad x_{k4}=(kf_4-f_3)w_3R_2^{-2k-2},$$

$$x_{k5}=R_1^2(s_5-s_7)+R_2^2(t_{14}-t_9),$$

$$x_{k6}=\big[(k+1)t_5+k(k+1)t_6-t_7+kt_8 +k(k-1)(k+1)t_{10}-k(k+2)t_{15}\big]R_2^{-2k+2},$$

$$x_{k7}=s_9-\left(k^2+2k-1\right)t_{10}+kt_{11},$$

$$x_{k8}=t_5+kt_6+k(k-1)t_{10},$$

$$x_{k9}=(e_1-ke_2-e_3)(k-1)w_1R_1^{2k},$$

$$x_{k10}=-kw_1e_3+(k-1)(k+1)w_1e_2-w_3f_2,$$

$$x_{k11}=(e_1-ke_2)w_1R_1^{2k-2}, \quad x_{k12}=-(k-1)w_1e_2R_1^{-2},$$

$$x_{k13}=\big[(k-1)s_1-k(k-1)s_2+s_3+ks_4 -k(k-1)(k+1)s_7-k(k-2)s_{11}\big]R_1^{2k+2},$$

$$x_{k14}=R_1^2(k+1)\big[\left(k^2-2k-1\right)s_7-ks_8-s_6-ks_{11}+\big] +R_2^2(k+1)(t_{14}-t_4),$$

$$x_{k15}=[s_1-ks_2-k(k+1)s_7]R_1^{2k},$$

$$x_{k16}=ks_8-\left(k^2-2k-1\right)s_7-t_{14}, \quad x_{k17}=\overline{x_{k1}},$$

$$x_{k18}=\overline{x_{k2}}, \quad x_{k19}=\overline{x_{k3}}, \quad x_{k20}=\overline{x_{k4}}, \quad x_{k21}=\overline{x_{k5}},$$

$$x_{k22}=\overline{x_{k6}}, \quad x_{k23}=\overline{x_{k7}}, \quad x_{k24}=\overline{x_{k8}}, \quad x_{k25}=\overline{x_{k9}},$$

$$x_{k26}=\overline{x_{k10}}, \quad x_{k27}=\overline{x_{k11}}, \quad x_{k28}=\overline{x_{k12}}, \quad x_{k29}=\overline{x_{k13}},$$

$$x_{k30}=\overline{x_{k14}}, \quad x_{k31}=\overline{x_{k15}}, \quad x_{k32}=\overline{x_{k16}},$$

$$u_{k1}=1/kw_3f_1\left(z_2^{-k}-z_1^{-k}\right),$$

$$u_{k2}=R_2^2\left(-1/kt_1z_1^{-k}+1/kt_1z_2^{-k}+t_2z_1^{-k}-t_3z_2^{-k}\right),$$

$$u_{k3}=\overline{u_{k1}}, \quad \text{and} \quad u_{k4}=\overline{u_{k2}}.$$

References

[1] Zhou K, Hoh H J, Wang X, Keer L M, Pang J H L, Song B and Wang Q J 2013 *Mech. Mater.* **60** 144

[2] Zhan G D, Kuntz J D, Wan J and Mukherjee A K 2002 *Nature* **2** 38

[3] Fu W Q, Wei Y, Zhu F, Liu L, Jiang K L, Li Q Q and Fan S S 2010 *Chin. Phys. B* **19** 088104

[4] Chen H, Chu K, Jia C, Liang X, Guo H and Qu X 2011 *Mater. Sci. Technol.* **27** 713

[5] Feng D L, Feng Y H, Chen Y, Li W and Zhang X X 2013 *Chin. Phys. B* **22** 016501

[6] Chopra N G, Luyken R J, Cherrey K, Crespi V H, Cohen M L, Louie S G and Zettl A 1995 *Science* **269** 966

[7] Zhang Z H, Guo W L and Dai Y T 2009 *J. Appl. Phys.* **105** 084312

[8] Wang Y L, Zhang J P, Su K H, Wang X, Liu Y and Sun X 2012 *Chin. Phys. B* **21** 060301

[9] Pan R J, Wu Y C and Liew K Y 2010 *Appl. Surf. Sci.* **256** 6564

[10] Zhang T H, Piao L Y, Zhao S L, Xu Z, Wu Q and Kong C 2012 *Chin. Phys. B* **21** 118401

[11] Iijima S 1991 *Nature* **354** 56

[12] Thess A, Lee R, Nikolaev P, Dai H J, Petit P, Robert J, Xu C, Lee Y H, Kim S G, Rinzler A G, Colbert D T, Scuseria G E, Tománek D, Fischer J E and Smalley R E 1996 *Science* **273** 483

[13] Qian D, Wagner G J, Liu W K, Yu M F and Ruoff R S 2002 *Appl. Mech. Rev.* **55** 495

[14] Luo Y P, Tien L G, Tsai C H, Lee M H and Li F Y 2011 *Chin. Phys. B* **20** 017302

[15] Sun Y F, Sun J D, Zhang X Y, Qin H, Zhang B S and Wu D M 2012 *Chin. Phys. B* **21** 108504

[16] Wang Y, Zhao Y J and Huang J P 2012 *Chin. Phys. B* **21** 076102

[17] Volterra V 1907 *Ann. Ecole Normale Sup. Paris* **24** 401

[18] Romanov A E and Vladimirov V I 1992 *Dislocations in Solids* Vol. 9 (Amsterdam: Elsevier Science Publishers B.V.) p. 191

[19] Romanov A E 1993 *Mater. Sci. Eng. A* **164** 58

[20] Murayama M, Howe J M, Hidaka H and Takaki S 2002 *Science* **295** 2433

[21] Fang Q H, Liu Y W, Jiang C P and Li B 2006 *Eng. Fract. Mech.* **73** 1235

[22] Qi W K, Zhu T, Chen Y and Ren J R 2009 *Chin. Phys. B* **18** 1002

[23] Zhou K and Wu M S 2010 *Int. J. Eng Sci.* **48** 237

[24] Kleman M 1983 *Points, Lines and Walls* (New York: Wiley-Interscience) pp. 220–224

[25] Hudson S D 1998 *Curr. Opin. Colloid Interface Sci.* **3** 125

[26] Klimanek P, Klemm V, Romanov A E and Seefeldt M 2001 *Adv. Eng. Mater.* **3** 1438

[27] Nye J F 1983 *Proc. R. Soc. A* **387** 105

[28] Chou T W and Malasky H J 1979 *Geophys. Res. B* **84** 6083

[29] Parameswaran V R 1979 *Specul. Sci. Technol.* **4** 509

[30] Zhou K, Nazarov A A and Wu M S 2008 *Philos. Mag.* **88** 3181

[31] Romanov A E 2003 *Eur. J. Mech. A. Solids* **22** 727

[32] Song H P, Fang Q H and Liu Y W 2010 *Chin. Phys. B* **19** 056102

[33] Birringer R and Gleiter H 1988 *Advances in Materials Science, Encyclopedia of Materials Science and Engineering* Vol. 1 (Oxford: Pergamon) pp. 339–349
[34] Gleiter H 1989 *Progr. Mater. Sci.* **33** 223
[35] Gutkin M Y and Ovid'ko I A 2003 *Rev. Adv. Mater. Sci.* **4** 79
[36] Gryaznov V G and Trusov L I 1993 *Prog. Mater. Sci.* **37** 289
[37] Romanov A E 1998 *Nanostructured Materials: Science and Technology* (Dordrecht Boston London: Kluwer Academic) pp. 207–242
[38] Gutkin M Y, Ovid'ko I A and Pande C S 2001 *Rev. Adv. Mater. Sci.* **2** 80
[39] Gryaznov V G and Trusov L I 1993 *Prog. Mater. Sci.* **37** 289
[40] Wu M S, Zhou K and Nazarov A A 2007 *Phys. Rev. B* **76** 134105
[41] Song H P, Fang Q H and Liu Y W 2008 *Chin. Phys. B* **17** 4592
[42] Luo J, Xiao Z M and Zhou K 2009 *Int. J. Eng Sci.* **47** 811
[43] Feng H, Fang Q H, Zhang L C and Liu Y W 2013 *Int. J. Plast.* **42** 50
[44] Kolesnikova A L, Romanov A E and Ovid'ko I A 2002 *Solid State Phenom.* **87** 265
[45] Ovid'ko I A, Sheinerman A G and Skiba N V 2003 *J. Phys.: Condens. Matter* **15** 1173
[46] Shodja H M, Gutkin M Yu and Moeini-Ardakani S S 2011 *Phys. Status Solidi B* **248** 1437
[47] Moeini-Ardakani S S, Gutkin M Yu and Shodja H M 2011 *Scripta Mater.* **64** 709
[48] Gurtin M E and Murdoch A I 1975 *Arch. Ration. Mech. Anal.* **57** 291
[49] Gurtin M E, Weissmuller J and Larche F 1998 *Philos. Mag. A* **78** 1093
[50] Fang Q H and Liu Y W 2006 *Acta Mater.* **54** 4213
[51] Fang Q H and Liu Y W 2006 *Scripta Mater.* **55** 99
[52] Liu Y W and Fang Q H 2007 *Mater. Sci. Eng. A* **464** 117
[53] Fang Q H, Liu Y W, Jin B and Wen P H 2009 *Int. J. Solids Struct.* **46** 1539
[54] Luo J and Liu F 2011 *Eur. J. Mech. A. Solids* **30** 22
[55] Ahmadzadeh-Bakhshayesh H, Gutkin M Yu and Shodja H M 2012 *Int. J. Solids Struct.* **49** 1665
[56] Shodja H M, Ahmadzadeh-Bakhshayesh H and Gutkin M Yu 2012 *Int. J. Solids Struct.* **49** 759
[57] Luo J and Xiao Z M 2009 *Int. J. Eng Sci.* **47** 883
[58] Muskhelishvili N L 1975 *Some Basic Problems of Mamatical Theory of Elasticity* (Groningen: Noordhoff International Publishing) pp. 64–118
[59] Liu Y W, Fang Q H and Jiang C P 2006 *Phys. Status Solidi A* **23** 443
[60] Fang Q H, Liu Y W, Liu Y and Huang B Y 2008 *Mater. Lett.* **62** 3521
[61] Sharma P, Ganti S and Bhate N 2003 *Appl. Phys. Lett.* **82** 535
[62] Fang Q H, Li B and Liu Y W 2007 *Phys. Status Solidi B* **244** 2576
[63] England A H 1971 *Complex Variable Method in Elasticity* (New York: Wiley-Interscience) pp. 110–125
[64] Xiao Z M, Yan J and Chen B J 2004 *Acta Mech.* **172** 237
[65] Zhang J F 2002 *Chin. Phys.* **11** 651
[66] Fang Q H, Liu Y W and Wen P H 2008 *J. Appl. Mech.* **75** 041019
[67] Ruud J A, Witvrouw A and Spaepen F 1993 *J. Appl. Phys.* **74** 2517